

Implementation of a Frequency Shift Correction Algorithm for Passive Coherent Location (PCL) Radar



Shi-Huan Eric Chen

A dissertation submitted to the Department of Electrical Engineering,
University of Cape Town, in fulfilment of the requirements
for the degree of Bachelor of Science in Engineering.

Cape Town, October 2008

Declaration

I declare that this undergraduate thesis is my own, unaided work. It is being submitted for the degree of Bachelor of Science in Engineering in the University of Cape Town. It has not been submitted before for any degree or examination in any other university.

Signature of Author

Cape Town

21 October 2008

Abstract

Receivers of Passive Coherent Location radar systems comprises of separate channels. A reference channel for receiving the direct signal from the transmitter and a surveillance channel for receiving echo signals from targets. The signals received from these channels are cross-correlated to estimate the range of the target as well as the Doppler-shift. A relative frequency drift between the channels will introduce an additional Doppler shift thus introducing errors in the speed and distance calculations of the target. This artificial Doppler will degrade the coherency of the radar system. This research project will investigate the effects of frequency drifts on the performances of passive radars. Characterization methods will be investigated and used to model and predict the frequency drifts, thus ultimately implementing corrective protocols to reduce the effects of frequency drifts.

Acknowledgements

I would firstly like to thank my supervisors, Professor Mike Ingg and Doctor Yoann Paichard, for their immense wisdom and guidance, as well as their patient supervision, which has enabled me to complete this research. Special thanks to all the master students in the Radar and Remote Sensing Group for their guidance.

I would lastly like to thank my family and friends for their support through this period.

Contents

Declaration	i
Abstract	ii
Acknowledgements	iii
List of Symbols	xi
Nomenclature	xiii
1 Introduction	1
1.1 Background	1
1.2 Scope and Limitation	2
1.3 Objectives	2
1.4 Plan of Development	3
2 Literature Review	5
2.1 Overview of Bistatic Radar Systems	5
2.1.1 Definition of Bistatic System	5
2.1.2 Modes of Operation	6
2.1.3 Synchronisation Methods	6
2.1.4 Advantages and Disadvantages of Bistatic Systems	7
2.1.5 Illuminators of Opportunity	7
2.2 Passive Coherent Location Radar Systems	7
2.2.1 System Overview of PCL	8
2.2.2 Advantages and Disadvantages of PCL Systems	11
2.2.3 Brief History on PCL Systems	11
2.2.4 Applications	12



2.2.5	Typical Illuminators	12
2.2.6	Doppler Resolution	14
2.3	Frequency Stability	15
2.3.1	Phase-Locked Loops	15
2.4	Summary	16
3	Software Defined Radio	17
3.1	Introduction	17
3.2	Software Radio	17
3.2.1	Front End of Software Radio	17
3.2.2	Applications of Software Radio	19
3.2.3	Framework and Tools for Software Radio	19
3.2.4	SDR Receiver Architecture	19
3.3	Universal Software Radio Peripheral	21
3.3.1	FX2 USB 2 Controller	21
3.3.2	ADC and DAC	21
3.3.3	FPGA	23
3.3.4	Daughter Boards	24
3.4	GNU Radio	25
3.4.1	Software Architecture	25
3.4.2	Hardware	26
3.5	Summary	26
4	Oscillator and Frequency Stability	28
4.1	Introduction	28
4.2	Quartz Crystal Oscillator	28
4.2.1	Dependence on Temperature	29
4.2.2	Long-Term Dependence on Time (Ageing)	29
4.2.3	Short-Term Dependence on Time	29
4.2.4	Types of Crystal Oscillators	30
4.2.5	Performance of Quartz Crystal Oscillators	30
4.2.6	Warm-Up Effect	31
4.3	System Setup	31
4.3.1	Results	33
4.4	Summary	37



5	Frequency Drift Characterization	39
5.1	Introduction	39
5.2	Frequency Domain Characterization	39
5.2.1	Drift Characterization	40
5.2.2	Relative Drift of Two Channels	41
5.2.3	State of Oscillators Over Long Periods	44
5.3	Time Domain Characterization	45
5.4	Results	47
5.5	Summary	51
6	Effects of Oscillator Mismatch	53
6.1	Introduction	53
6.2	Doppler Effect	53
6.3	Cross-Correlation	55
6.4	Results	56
6.5	Summary	59
7	Conclusions and Future Work	61
A	Frequency Measurements	63
B	Cross-Correlation Plots	66
C	Images of Equipment	69
D	Software Codes	73
D.1	Python codes	73
D.2	Matlab codes	73
D.3	FERS Simulator [8]	74
	Bibliography	75

List of Figures

2.1	Block diagram of PCL system	9
3.1	Typical block diagram of Software Radio front end	18
3.2	Block diagram of USRP and daughter boards [7]	21
3.3	Receiver system overview	22
3.4	DDC block diagram [7]	24
3.5	Block diagram of flow graph [29]	26
4.1	Block diagram of experimental setup	32
4.2	Frequency positions at start of the experiment	33
4.3	Frequency positions at start of experiment (zoomed)	34
4.4	Frequency drift of both channels and relative frequency shift	34
4.5	Frequency drifts of both channels and relative frequency shift over one hour	35
4.6	Frequency drifts of both channels over 1 minute	36
4.7	Offset between channels	36
4.8	Position of peaks over one minute	37
5.1	Categories of phase noise corresponding to power law spectra [9]	46
5.2	Frequency of both channels (Start up)	47
5.3	Frequency of both channels (Stable conditions)	47
5.4	Phase of frequencies of figure 5.2	48
5.5	Phase of frequencies of figure 5.3	48
5.6	Phase model of channel A	49
5.7	Phase model of Channel B	50
5.8	Drift in peak of FFT	50
5.9	Model of relative phase between channels	51
6.1	Concept of cross-correlation [22]	55



6.2	Cross-correlation of the reference and echo signals	57
6.3	Colour map of ideal signal cross-correlation	57
6.4	Effects of frequency offset	58
6.5	Effects of frequency drifts	58
6.6	Actual results based on predictions	59
A.1	Relative frequency during 10:45 am	63
A.2	Relative frequency during 11:45 am	65
A.3	Relative frequency over 1hr measurement	65
B.1	Cross-correlation with frequency offset	66
B.2	Contour plot with frequency offset	67
B.3	Cross-correlation plot with frequency drift	67
B.4	Contour plot with frequency drift	68
C.1	USRP board	70
C.2	USRP with TVRX Daughter boards	71
C.3	USRP and signal generator	71
C.4	USRP and GPSDO	72

List of Tables

- 4.1 Typical ageing rates (Long-term) 31
- 4.2 Typical short-term stability rates 31

- A.1 Measurement of frequency shifts 64

List of Symbols

f_d	– Doppler frequency shift
v_r	– Radial velocity of the target with respect to the radar
f_0	– Transmitted frequency
Δf_d	– Doppler resolution
δf_d	– Accuracy of Doppler resolution
N	– Number of bits of resolution of the ADC
f_s	– Sampling rate of the ADC
B	– Bandwidth of the signal
T	– Time gate over which the frequency is averaged
V_0	– Nominal peak voltage
$\varepsilon(t)$	– Deviation of the amplitude from nominal
$\Phi(t)$	– Total oscillator phase
$\phi(t)$	– Deviation of the phase from the nominal
$x(t)$	– Time (phase) error of the oscillator
a	– Initial time offset
b	– Initial frequency offset
D_r	– Frequency drifts
$\varepsilon(t)$	– Random deviations
S_1	– Respective amplitude of signal 1
S_2	– Respective amplitude of signal 2
$\varphi_1(t)$	– Instantaneous phase 1
$\varphi_2(t)$	– Instantaneous phase 2
$\phi_1(t)$	– Residual phase 1
$\phi_2(t)$	– Residual phase 2
\mathbf{X}_1	– 1-column array 1
\mathbf{X}_2	– 1-column array 2
\mathbf{T}	– 1-column array of the corresponding sampling times
\mathbf{I}	– Identity matrix (1 in diagonal, 0 elsewhere)
\mathbf{T}^τ	– Transposed (1-line) array of \mathbf{T}
x_n	– Equivalent to $x(n\tau_0)$

- τ_0 – System sample rate
- σ^2 – Standard deviation
- R – Range of the target from the radar
- τ_d – Round trip time delay of the signal between transmitter and receiver
- c – Propagation speed
- R_T – Range of the transmitter to the target
- R_R – Range of the target to the receiver
- Ψ – Amplitude-range-Doppler (ARD)
- $e(n)$ – Filtered echo signal
- $d(n)$ – Reference signal
- τ – is the time delay corresponding to the bistatic time difference of arrival
- ν – Doppler shift of interest

Nomenclature

Doppler frequency—A shift in the radio frequency of the return from a target or other object as a result of the object's radial motion relative to the radar.

PRF—Pulse repetition frequency.

Range—The radial distance from a radar to a target.

Phase noise—Frequency domain representation of rapid, short-term, random fluctuations in phase

Time delay—The delay in time for a signal traveling from transmitter to target to receiver, compared to transmitter to receiver

Resolution—The minimum spacing between two targets which allows them to be distinguished, by the radar.

SNR—Signal to noise ratio

LO—Local oscillator

IF—Intermediate frequency

FM—Frequency modulation

PM—Phase modulation

Chapter 1

Introduction

1.1 Background

Passive radar systems are used in the detection and tracking of objects by processing the reflections from these objects or other sources of illumination within the environment. A basic, well known form of passive radar systems is the bistatic radar whereby the transmitter and receiver is not collocated. The transmitter and receiver of a bistatic radar system is separated by a certain amount that is comparable to the maximum expected range of the target to be detected.

In active radar systems, whereby transmitter and receivers are collocated, the transmit frequency and waveform are exactly known, thus target range and speed may be easily calculated to a great deal of accuracy. In passive radars the transmitted information is not directly accessible, thus it uses two separate channels to process the signals. The first channel is used for processing the direct signal from the transmitter of opportunity which is then used as a reference for the receiver. The second channel receives the echo signal that is reflected by the target or object of interest. Then, by cross-correlation of the time differences between the reference and reflected signal, the bistatic range of the object may be determined. It can also typically measure the bistatic Doppler shift and the direction of arrival. The target may be moving, thus the reflected signal is Doppler shifted in frequency depending on its velocity and bistatic angle between the transmitter and receiver. This will allow for speed, heading and distance of the object to be calculated.

The main difficulty with having two separate channels is the synchronisation between the two channels. Channels that are not synchronised creates frequency offsets, and frequency drift in the received signals, thus introducing an additional Doppler shift. Consequently, this additional Doppler shift introduces errors in speed and distance calculations of the object. In addition, if fully coherent processing is attempted, there will be degradation to the coherency due to this artificial Doppler.

This thesis reviews some literature on relevant topics to this thesis and investigates the effects of mismatched receiver channels as well as relative frequency drift characteristics. These effects and characteristics will be modelled in simulation and results will be presented and discussed in detail.

1.2 Scope and Limitation

The main limitation of this research project is time due to the fact that, to accurately characterize the frequency drifts, long-term (days, months or years) characterization is required. Frequency stability is dependent on local oscillators, thus the stability of oscillators need to be investigated over short-term and long-term periods. Another limitation is the processing of large amounts of data. There are sampling rate limitations in the equipment used, thus sampling continuously over long periods of time will result in large data files that are just too large to be processed.

The scope of this project will cover the characteristics of frequency drifts by investigating the phase and briefly discussing the effects of phase noise on the stability. The properties of quartz oscillators will be investigated, and their effects on frequency drift. Characterization methods of the frequency drifts will be examined and used for predictions of drift, and the effects of this drift on passive radar systems.

1.3 Objectives

The objectives of this research project are:

- To review and research literature related to the topic
- To record two channels of real time FM signals over a specified length of time
- To process these signals and evaluate the frequency drift between the two channels
- Model the time, frequency and phase of the signal using characterization techniques
- Measure and model the Doppler shift involved by the receivers
- Simulate and implement a frequency shift correction
- Draw conclusions and recommendations from the research

These objectives are essentially fairly broad and each objective will be stated clearly in the chapters as well as the methods of investigation and analysis.

1.4 Plan of Development

Chapter 1 forms the introductions to this project. Background to this research is discussed, presenting the problem at hand and defining the objectives of this thesis. Scope and limitations are mentioned and the plan of development is discussed.

Chapter 2 is the literature review, investigating previously published material and presenting information that is relevant to this project. This chapter begins with a brief background to active and passive radar systems. An overview of bistatic radar systems is discussed, noting that the transmitter and receiver are not collocated. Thus, the modes of operation is defined into three categories namely, dedicated, cooperative and non-cooperative. Due to the separation of the transmitter and receiver, synchronisation methods are discussed.

Illuminators of opportunity is introduced, thereafter an overview of PCL radar systems is investigated, mentioning some advantages and disadvantages of using illuminators of opportunity. Distinction between the application of PCL radar systems are mentioned. History of PCL systems is briefly discussed as well as its developments and research. Typical illuminators are mentioned, with broadcasting transmitters being the most popular, due to its inherent properties of high transmit powers and wide coverage.

This chapter ends with a brief outline to frequency and timing stability. This will introduce concepts and topics that are relevant to this project and will be covered in later chapters.

Chapter 3 covers the use of software radio. Software radio is initially defined, and a thorough overview of software radio is made, including discussions of its applications, framework and architecture. The USRP will be used for experimentations in this research, and thus the system overview will be investigated. Focus will be made on each component of the USRP board.

GNU Radio is a free toolkit, open source software platform used for building and developing software defined radio systems. Fundamentally it is a signal processing package used to access the electromagnetic spectrum. The software architecture is discussed as well as mentioning compatible hardwares. The USRP is a popular choice for use with GNU Radio.

Chapter 4 introduces oscillators and covers a thorough overview of the quartz crystal oscillator, its dependencies on time as well as environment. The different types of crystal oscillators are listed and specifying their performances and stability over long-term (ageing) and short-term periods.

Thereafter, the stability of the oscillators within the USRP daughter boards is investigated, by sending a common signal to two daughter boards. This is used to model the separate channels in a passive radar receiver. Frequency measurements are then taken over time for specified time durations. The frequencies are then compared with each other to calculate the frequency shift between the two sig-

nals. These are carried over to the following chapters.

Chapter 5 discusses frequency characterization methods to model the performances of the oscillators. Characterization of frequency properties will focus on the phase of signals as well as evaluating the relative phase between two signals. The frequency offset and frequency drifts can be determined through phase characterization. The Allan variance, used to measure the stability of oscillators, is presented. Allan variance can also typically measure the phase noise of a signal.

By taking advantage of its stability, a GPSDO [14] is used for experimentations to measure the relative drifts between two signals. Models of the phase and frequency characteristics are made and used for prediction.

Chapter 6 presents the effects of oscillator mismatch. These mismatches are typically in the form of frequency offset and frequency drifts. The relationship between timing errors and the target range is briefly discussed. The cross-correlation process in passive radars is presented in detail, showing that the process acts like a matched filter for radar systems. The mismatch effects are shown in results, and discussed, relating to the overall system performance.

Chapter 7 describes the conclusions drawn from the work completed, and looks into further improvements and future work.

Chapter 2

Literature Review

The following chapter reviews some literature on subjects that are relevant to this research project. Basic principles of radar systems will be discussed whilst focusing on radar receivers. Signal processing and matched filtering will be examined, and oscillator mismatch effects will be investigated. A brief history about Passive Coherent Location radar systems will be discussed. These discussions and investigations will form the basis of this project.

2.1 Overview of Bistatic Radar Systems

Initially radar systems were built with bistatic characteristics, whereby the transmitters and receivers were separated by a certain distance. Technological advancements in the form of the duplexer has allowed the transmitters and receivers to be collocated, sharing a common antenna and site [32]. This simplifies operations as well as savings on costs and space, thus monostatic radars have dominated radar research and design. Although bistatic radars have certain advantages over monostatic radars, their disadvantages had previously outweighed their advantages, in particular the complexities of synchronization between transmitter and receivers, as well as receiver channels [4].

With technological improvements in the form of high speed digital signal processors (DSP) and the deployments of Global Positioning Systems (GPS), which may be used for synchronization, have allowed these complexities to be mitigated, thus renewing interests in bistatic radar systems.

2.1.1 Definition of Bistatic System

Radar systems whereby the transmitter and receiver is collocated, or located on the same site, is considered a monostatic radar system, also known as “Quasi-bistatic”. If the transmitter and receiver is separated by a distance that is comparable to the distance of the target, this systems can be de-

defined as bistatic. A bistatic system utilizes the reception, acquisition, processing and analysis of the illuminating signal scattered by the target to determine the target's location, velocity, tracking etc.

2.1.2 Modes of Operation

Bistatic radar systems can operate in three different modes [33], namely:

- **Dedicated:** This dedicated mode of operation is defined as being under both the design as well as the control of the bistatic system.
- **Cooperative:** This system is basically designed for other functions or applications, but is suitable for bistatic operations and the transmitter can be controlled to do so.
- **Non-cooperative:** This system is designed for other functions or applications, that is suitable for bistatic operation, but the transmitter cannot be controlled.

2.1.3 Synchronisation Methods

Due to the nature of these modes of operation and the separation of the transmitter and receiver, synchronisation between the transmitter and receiver must be maintained. In order to determine the location of the target as several aspects need to be known, such as the elevation, transmit azimuth and timing of the transmitted signal. The transmitted waveform must be available for matched filter operations, as well as the phase of the waveform for coherent receiver operations. Thus the synchronisation between the transmitter and receiver is crucial towards the accuracy of the system [12, 33]. This may be achieved in the following methods:

- **Direct synchronisation:** This method uses a signal, sent from the transmitter to the receiver, to synchronise a clock which allows for timing accuracy. Various methods may be used for this type of synchronisation such as the use of a land line, a communication link, or the receiver may be directly synchronised at the transmitters RF if an adequate line-of-sight exists between the transmitter and receiver.
- **Indirect synchronisation:** This method of synchronisation is achieved by using identical clocks that have been stabilised at both the transmitting and receiving sites. However, the clocks must be periodically monitored and synchronised.
- **Direct breakthrough synchronisation:** This is achieved when the transmitting beam scans past the receiving site, and given an adequate line-of-sight, the receiver then synchronises to the transmitter on the pulses received during the main beam illumination period.

2.1.4 Advantages and Disadvantages of Bistatic Systems

The principal advantages of bistatic radars are [4]:

- Far less vulnerable to electronic counter measures (ECM) due to the passive nature of the receivers
- It is a counter stealth technology, designed primarily to defeat monostatic radars
- Employment of a multistatic system (Multiple receivers, forming a bistatic radar with a single transmitter) offers greater and customized coverage, and a richer information source enabling more accurate detection, tracking and target reconstruction.

However, the disadvantages are:

- Increased system complexity and processing compared to monostatic systems
- Synchronisation and beam pointing are difficult to implement

Although bistatic configurations may introduce certain disadvantages and more complexities than that of a monostatic system, there are great strategic and economical advantages to using a bistatic system, and now more practical systems are beginning to emerge. With greater advancements in the technological field, bistatic radars have become increasingly popular with numerous applications.

2.1.5 Illuminators of Opportunity

More recently there has been an increase in the interest in bistatic radar systems that exploit illuminators of opportunity. This is also known as a Passive Coherent Location (PCL) radar system. This system can dramatically reduce the costs in system hardware. With the rapid growth in the number of RF emissions for radio and TV broadcasting, as well as the increase in terrestrial and space based communications, a wide range of signal types are available for exploitation by passive radars. Further, many of these transmissions are at VHF and UHF frequencies, thus allowing these parts of the spectrum, which are not normally used for radar, to be used. However the transmitter's location and transmission properties are no longer under the control of the radar designer [4].

2.2 Passive Coherent Location Radar Systems

Passive Coherent Location (PCL) radar systems is a special case of a bistatic configuration which exploits transmitters of opportunity, usually radio or TV broadcasting transmitters. Radar designers have no control over these transmitters, its location, transmitted waveform properties or timing information related to the transmission, therefore the use of a dedicated receiver (Reference channel) is required to monitor each transmitter being exploited.

2.2.1 System Overview of PCL

This section will provide the reader with some general information and insight into the workings as well as the implementation of the overall PCL system, without providing large amounts of detailed theory.

To ensure the ability to detect and track targets accurately, a passive radar typically consists of several hardware systems and the following processing steps¹ [22, 13]:

- Reception of the direct signal as well as the echo signals, scattered by the target over the surveillance region, from the transmitter on a dedicated low-noise, linear, digital receivers
- Transmitter signal conditioning to improve the reference signal
- Adaptive filtering to cancel out any unwanted signal interference between the channels
- Determine the target's bistatic range and Doppler by cross-correlation of the receiver channels
- Detection using a *constant false alarm rate* (CFAR) scheme
- Association plot data with individual targets, conventionally using a Kalman filter. This is known as "Line tracking".
- Association of line tracks to form final estimate of a targets location, heading and speed

Receiver System

Passive radar receivers usually consists of two separate channels, one to process the reference signal and the other to process the echo signals from targets. Thereafter, cross-correlation processing is used to determine properties of the target. Due to the nature of PCL systems using illuminators of opportunity, whereby they must detect very small target returns in the presence of continuous and significant interference, it is essential that the PCL receivers should have a low noise figure, high dynamic range and high linearity. In order to achieve the processing gain necessary to detect these weak target returns in a background of noise and interference it is necessary to process the signal through a matched filter. A matched filtering process is used to maximize the SNR, and by passing target echoes through a matched filter, it is equivalent to the correlation of the radar echo with a delayed replica of the transmitted signal which is obtained via the reference channel [13].

The greatest source of interference, and hence the limitations on the system performance, is the *Direct Path Interference* (DPI) received form the transmitter. This unwanted DPI signal correlates with

¹Refer to figure 2.1

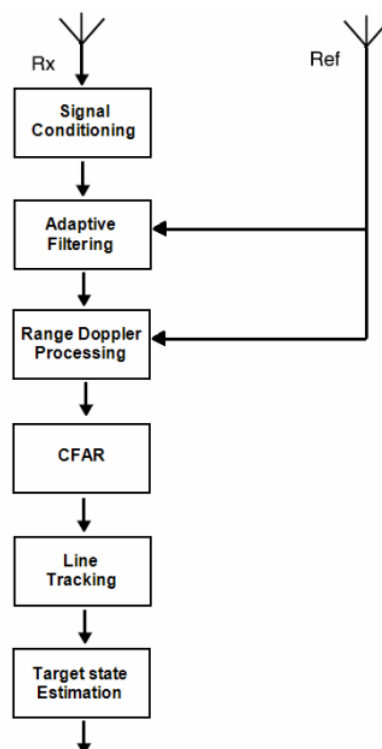


Figure 2.1: Block diagram of PCL system

the reference signal and produces range and Doppler sidelobes that are several orders of magnitudes greater than the echoes [17]. To detect targets that may be further away it is necessary to remove this signal by both angular nulling with antenna and adaptive echo cancellation in the receiver. Further interference is due to the co-channel interference coming from other transmissions operating at the same frequency within a single frequency network. This co-channel interference has similar effects as that of the DPI. In addition, the signal is always received against a background of reflections from the surface, known as clutter, and could be buried under these interferences.

Signal Conditioning

With certain transmitter types, it is necessary to perform some transmitter-specific conditioning of the signal before cross-correlation processing. This may include high quality analogue bandpass filtering of the signal, channel equalization to improve the quality of the reference signal and removal of unwanted signals. This may improve the radar ambiguity function or even complete reconstruction of the reference signal from the received digital signal.

Adaptive Filtering

The main limitation in the detection of target range for most passive radar systems is the *Signal to Interference Ratio* (SIR), due to the large and constant direct signal received from the transmitter.

An adaptive filter can be used to remove this direct signal, and is essential to ensure that the range or Doppler sidelobes of the direct signal do not mask the smaller echoes in the subsequent cross-correlation process stage.

Cross-correlation

Cross-correlation is the main processing step in a passive radar. It is the measure of the similarity of two waveforms as a function of a time-lag applied to one of them. This step acts as the matched filter to provide the necessary processing gain, thus maximising SNR. This process also provides the estimates of the bistatic range and the bistatic Doppler shift of each target echo. Cross-correlation will be discussed in more detail in section 6.3.

Most analogue and digital broadcast signals are noise like in nature, and as a consequence they tend to only correlate with themselves. This causes a problem with moving targets as the Doppler shift imposed on the echo means that it will not correlate with the direct signal from the transmitter. As a result, the cross-correlation processing must implement a bank of matched filters, each matched to a different target Doppler shift.

Target Detection

Targets are detected on the cross-correlation surface by applying an adaptive threshold, and declaring all returns above this surface to be targets. A standard cell-averaging CFAR algorithm is typically used and determines the range and Doppler of each target.

Line Tracking

At this stage of the signal processing the system has determined the range and Doppler of a number of targets. For further processing it is necessary to associate this plot data with individual targets and this is performed using a conventional Kalman filter. Most false alarms are rejected during this stage of the processing.

Track Association and State Estimation

After having associated the plots to the targets, the range and Doppler data for each target are processed by a non-linear estimator to determine the target's location, speed and heading. By using a non-linear estimator, it allows optimal use of the Doppler information in this tracking process.

2.2.2 Advantages and Disadvantages of PCL Systems

PCL systems inherits all the associated advantages and disadvantages of bistatic or multistatic systems, as PCL configurations are either bistatic or multistatic in nature.

PCL systems also includes the following advantages [13]:

- Low implementation costs as there are no transmitter hardware.
- Lower costs of operation and maintenance due to lack of transmitter and moving parts.
- Physically small, thus it may be easily deployed in places where conventional radars cannot operate due to its size.
- Covert operations, and no need for frequency allocations.
- Detect targets continuously, typically once a second.

The associated disadvantages of PCL systems are:

- A reliance on third-party transmitters, giving the radar designers and operators little control over the availability of the illuminators.
- Line of sight is required between the transmitter and receiver. This also imposes performance limitations and complexity of deployment due to DPI and co-channel interference.

2.2.3 Brief History on PCL Systems

Various early forms of radar devices, which were mainly used for detecting ships, were developed between 1903 and 1925. These radars were able to measure the distance (range) to a target besides the targets presence [18]. These early radars were all essentially bistatic configurations as there had been no development in technology to enable an antenna to be switched from transmit to receive mode [12].

The first non-cooperative bistatic system was built by the Germans during World War 2, and by 1936, with the invention of the duplexer, bistatic radar systems gave way to monostatic systems. Monostatic systems were easier to implement since they eliminated the geometric complexities introduced by the separate transmitter and receiver sites. In addition, aircraft and shipborne applications became possible as smaller components were developed [33].

During the 1950s, bistatic systems was revived, whereby the research primarily focused on theory and measurement, properties of the scattered radar energy and multistatic radars [33].

By the late 1970s, much of the early work published on PCL systems was conducted at University College London (UCL). A number of experimental bistatic systems have been built and evaluated by Schoenenberger, who designed and built a system using UHF Air Traffic Control radar at Heathrow airport as an illuminator, and investigating problems of synchronisation between transmitter and receiver. Proceeding work at UCL attempted to use UHF television transmission as illuminators of opportunity to detect aircraft taking off and landing from Heathrow airport [27].

Howland [22] developed a UHF forward scatter system based on television transmissions. Further work by Howland investigated the use of FM radio broadcast transmissions, which closely resembles his previous work based on television transmissions, employing Doppler, range and bearing data [15].

Research on PCL radar systems is of growing interest throughout the world, with various open source publications showing active research and development, and are now currently under development in several commercial organizations [22].

2.2.4 Applications

There are several reported applications of PCL systems, including:

- Air-space surveillance
- Atmospheric and ionospheric studies
- Oceanography and maritime surveillance
- Detection of radioactive pollution
- Mapping lightning channels in thunderstorms

There are also reports and documentation of possible tornado detection and tracking using PCL radar systems. There is a growing diversity of PCL applications and is indicative of the increasing importance of PCL radar systems.

2.2.5 Typical Illuminators

There is a wide range of RF emissions, such as radio and TV broadcasts as well as terrestrial and space based communications has resulted in a wide range of signal types available for exploitation by passive radars.

Typical sources include:

- FM radio signals
- Analogue TV signals
- GSM base stations
- Digital Audio and Video Broadcasts
- Terrestrial HDTV

With the wide range of transmitters of opportunity available in the environment, broadcast transmitters are some of the most popular transmitters used for surveillance purposes, because of their inherent attractive properties of very broad coverage and relatively high transmitter powers.

Satellite signals are generally inadequate for passive radar use, as their transmission powers are far too low, and have infrequent illumination due to their orbit paths.

Digital audio transmitters emit signal at higher frequencies than FM transmissions, however FM transmissions are comparatively higher in their power. Thus, the maximum detection ranges offered by FM transmissions are greater than that of Digital audio [3]. Furthermore, the coverage of Digital audio is generally poor because these networks are still expanding and may be non-existent in certain countries.

Cellular phone base stations transmit at rather low power, but there is an extensive network and targets could be tracked through such a network, thus coverage may be extended greatly. This however comes with increased system complexity, and furthermore, the base stations deliberately concentrate emissions towards the ground and may not necessarily have good coverage of higher altitudes.

FM transmission have been used for ionospheric studies [24] and therefore might be expected to have useful height surveillance. Their high powers and good coverage make FM radio transmissions particularly well suited for air target detection, both civil and military applications. They could also be used for marine navigation in coastal waters, though clutter will be a more significant problem.

Wideband processing in PCL systems is defined as the use of a receiver that has a bandwidth that is comparable to that of the waveform being processed. Typical FM radio broadcast occupies bandwidths of approximately 100kHz, thus offering a potential range of up to 1500m. However, as a result of this lower bandwidth available, range and bearing are a factor often or so worse than a conventional microwave radar. With Doppler it is two or three orders of magnitude more accurate, due to the extended integration times that are potentially achieved by passive radars. The resolution,

may thus be comparable to conventional radars by using the Doppler information, and may even achieve greater accuracies by simultaneously using multiple transmitters.

2.2.6 Doppler Resolution

Doppler is the relative change in radio frequency of the signal, caused by the relative motions of the target with respect to the receiver. To accurately measure the speed of the target the Doppler shift must be used. With a moving target, the target to radar range as well as the phase of the radar signal are continuously changing. By using electromagnetic propagation theories this change in phase with respect to time is related to the Doppler angular frequency and can be shown in [19] that the Doppler frequency shift is given by:

$$f_d = \frac{2v_r}{\lambda} = \frac{2v_r f_0}{c} \quad (2.1)$$

Where:

- f_d is the Doppler frequency shift
- v_r is the radial velocity of the target with respect to the radar
- f_0 is the transmitted frequency

Equation 2.1 defines the Doppler frequency for a monostatic case. With a bistatic case the change in radio frequency is a result of the rate of change of the total path length travelled by the signal. In the monostatic case this change in path length is equal to a change in the targets range. For a bistatic system the Doppler shift is given by:

$$f_d = -\frac{1}{\lambda} \frac{d(R_T + R_R)}{dt} \quad (2.2)$$

Equation 2.2, indicates that there is a decrease in Doppler frequency for an increase in the path length [21]. In this case the Doppler frequency shift provide means of distinguishing between a stationary and a moving target, and is not a measure of the radial velocity as with the monostatic case.

The velocity resolution, which is the ability to separate two targets in Doppler is the same as with the Doppler resolution and can be expressed by:

$$\Delta f_d = \frac{1}{PRI} \quad (2.3)$$

Increasing the duration of the signal will allow resolution to become finer, and thus, a more accurate Doppler frequency shift can be determined.

From equation 2.3, the accuracy of the Doppler resolution is given by:

$$\delta f_d \simeq \frac{1}{PRI \cdot (\sqrt{2} \cdot SNR)} \quad (2.4)$$

Thus it is determined that longer duration waveforms permits velocity resolution and accuracy, whereas for range resolution and accuracy a short waveform is required.

2.3 Frequency Stability

A limiting factor in the performance of radar applications is the ability of the radar's frequency reference to maintain timing accuracy and frequency stability. This is especially crucial in passive radars due to the separation of the channels in receivers.

Oscillators² are key components in wireless transmitters and receivers, as they provide precisely controlled sources for frequency conversion. Thus, oscillator performances are directly proportional to the performances of a radar [19]. The frequency generated by any oscillator is subject to changes in the environment including temperature, mechanical and electrical disturbances, thermal noise etc. Long term drift (ageing) of the components produces changes in the circuit-transfer phase characteristics, which in turn produces corresponding long-term changes in the operating frequency. These long term effects may be the results of relaxation of electrode and mounting-system stresses, surface and subsurface changes and diffusion of metal electrode systems [5].

It is clear that the timing accuracy and frequency stability is dependent on the performances of oscillators. Timing and frequency instabilities will have direct effects on radars to accurately track targets and measure the Doppler shift of the targets. These effect will be discussed in chapter 6 as well as the effects of oscillator mismatch.

2.3.1 Phase-Locked Loops

A phase-locked loop (PLL) uses a feedback control circuit to allow a voltage controlled oscillator to precisely track the phase of a stable reference oscillator. The output oscillator of this system can be used to run at a multiple of the reference oscillator frequency. PLL are used as FM demodulators, in carrier recovery circuits, and as frequency synthesizers for modulation and demodulation. PLL systems have very good frequency accuracy and phase noise characteristics, but as a consequence, the settling times between changes in frequency can be long [19].

²Oscillators will be discussed in detail in Chapter 4.

2.4 Summary

This chapter briefly introduces bistatic radar systems and explores the concepts of PCL radar systems, noting that PCL are fundamentally bistatic in nature. PCL systems make use of non cooperative transmitters by exploiting these illuminators of opportunity, such as radio and TV broadcast transmissions and communication signals. Furthermore, PCL systems uses these signals to measure the difference in time of arrival as well as Doppler shifts between the direct signal from the transmitter and the echo signal reflected by the target. These measurements are used to locate the targets and track its speed and heading.

The PCL system overview is discussed, and mentioning some advantages and disadvantages of using illuminators of opportunity. Although the performances of bistatic radar systems does not rival that of the monostatic radar system, there are some distinct advantages and applications within bistatic systems which cannot be implemented with a monostatic system. An example of bistatic systems with distinct advantages and applications is the extremely low cost of design and implementation and can be used to detect stealthy aircrafts.

History of PCL systems is briefly discussed as well as its developments and research. Typical illuminators are mentioned, with broadcasting transmitters being the more favourable, due to its inherent properties of high transmit powers and wide coverage.

This chapter ends with a brief outline to frequency and timing stability and its importance to the performance of radars. This outline introduces concepts and topics that are relevant to this thesis and will be covered in the following chapters.

Chapter 3

Software Defined Radio

3.1 Introduction

With continuous technological innovations, and with the growing popularity of software systems, developments of new radio technologies have become possible. One such technology is the software defined radio. With the interests of software defined radio expanding and pushes ever widening frontiers, the Free Software Foundation (FSF) has developed and is maintaining a software defined radio project called GNU Radio. GNU Radio is a collection of software tools that when combined with minimal hardware, allows the construction of radios where actual waveforms are defined by software. These applications and signal processing can be implemented on a PC using external USB based hardware, known as the *Universal Software Radio Peripheral (USRP)*, which is also developed as part of the GNU Radio.

3.2 Software Radio

Software radio is a revolution in radio design due to its ability to create radios that are constantly changing, creating new choices for users. Software radio is the technique of modelling code as close to the antenna as possible, turning radio hardware problems to software problems. The fundamental characteristics of software radio is that software defines both the transmitted waveforms, as well as the demodulation of the received waveforms. Furthermore, signal processing is done in software rather than traditional radios which uses either analog circuitry or a combination of analog circuitry with digital chips [7].

3.2.1 Front End of Software Radio

SDRs have the ability to be transformed through the use of software and re-definable logic, which is achieved with general purpose digital signal processors (DSPs) or field programmable gate arrays

(FPGAs). SDRs have greater flexibility compared to traditional radios as channel bandwidth, rate and modulation are all determined through software. Thus, SDRs have the ability to go beyond simple single channel, single mode transceiver technology as well as the ability to change modes arbitrarily.

To make full use of these concepts, SDRs keep the signals in the digital domain for as much of the signal chain as possible, digitizing and reconstructing close to the antenna, thereby allowing digital techniques to perform functions done by analog components as well as the additional functions that are not possible in the analog domain. The waveforms are generated as sampled digital signals, which are then converted from digital to analog via a wideband DAC. Similarly, the receiver employs a wideband ADC that captures all of the channels of the software radio node. The receiver then extracts, down convert and demodulates the channel waveforms using software on a general purpose processor [20]. However, connecting ADCs and DACs directly to the antenna introduces concerns regarding the selectivity and sensitivity. Thus the need for a flexible analog front end that is capable of translating a wide range of frequencies and bands is required so that the data converters are able to adequately process the data [20].

SDRs uses digital filters, which can be altered, to determine the channel bandwidth. This provides SDRs with the resources to vary the bandwidth dynamically. Digital filters also have the potential to implement filters that are not possible in the analog domain and are able to compensate for transmission path distortion, which would be complex to implement using analog filters.

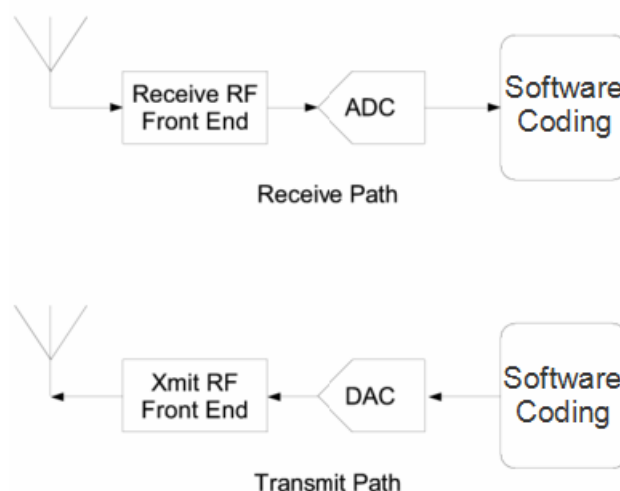


Figure 3.1: Typical block diagram of Software Radio front end

3.2.2 Applications of Software Radio

Software radio is finding use in an increasing number of applications. Software radio enables rapid prototyping and deployment of sophisticated wireless systems, making it ideal for a wide range of research areas and development applications in commercial and military.

Typical applications include:

- Battlefield, survivable and ad-hoc network
- Passive Coherent Radar
- Satellite communications
- Mine and underground communications
- Radio Astronomy
- Cognitive Radio

3.2.3 Framework and Tools for Software Radio

Several software radio environments are available, with common solutions such as:

- C/C++
- GNU Radio
- Matlab/Simulink/LabView
- JTRS
- OSSIE

3.2.4 SDR Receiver Architecture

The first element in the receiver chain is the antenna. A fully developed SDR usually has an antenna that is additionally a programmable component. Ideally, the SDR would have its ADC connected directly to the antenna of the receiver, this is in order to facilitate the implementation of as much of the system components in the digital domain. However, this is not a practical solution and some form of an analog front end must be used before the ADC in the receiver path in order to conduct the appropriate frequency translation. An example of this is the use of a *low-noise amplifier* (LNA) before the ADC as analog-to-digital converters lack the discrimination to pick up sub-microvolt, nanowatt

radio signals. However, the LNA device may introduce its own problems, such as spurious signals which may introduce distortion to desired signals or block them completely. A typical solution for this is to use a band-pass filter before the LNA, which then reduces the flexibility of a software radio [20].

The most common of these architectures is the super heterodyne architecture. In this instance the midrange IF produced by the receiver allows the use of sharper cut off filters for improved selectivity. Additionally higher IF gains are achieved through the use of IF amplifiers, improving sensitivity. The super heterodyne receiver uses two stages of conversion and is useful at microwave frequencies in avoiding problems associated with *local oscillators* (LO) instabilities [19].

Direct conversion architecture down-converts the RF signal to a zero IF frequency, with the use of a mixer and local oscillator. The local oscillator is set to the same frequency as the RF signal, which then converts directly to the baseband. The architecture has the advantage of being simpler to implement and less costly to build. Furthermore, direct conversion does not generate any image frequencies, since the mixer difference frequency is effectively zero, and the sum frequency is twice the LO and can be easily filtered. The main disadvantage is that the LO must have a very high degree of precision and stability to avoid drifting of the received signal frequency [19].

Mixers are used to translate the RF signal to a suitable IF frequency. A number of mixer stages may be used, as was described for the superheterodyne architecture. To eliminate undesired images as well as other undesired signals, filtering is made use of at each stage. A quadrature demodulator is sometimes employed in addition to, or instead of, a mixer. This is used in order to separate the I and Q components which undergo separate signal conditioning. Due to the digital nature of the receiver this is not a problem. However in the analog domain the signal paths must be perfectly matched, or I/Q imbalances will be introduced, potentially limiting the suitability of the system.

The ADC is used to convert the IF signal or signals into digital form for processing. The ADC defines the performances of the SDR receiver. It is common that the ADCs in the SDR receivers are over specified as their applications are unknown prior to their selection and the best available ADC is selected. There are several options to implement the digital processor. For very high sample and data rates, a FPGA is usually implemented, which are flexible in their functions and range of parameters. FPGAs may be used to program any function desired, in addition they are typically programmed to perform quadrature demodulation, tuning, channel filtering and data rate reduction among others. The FPGA is capable of implementing and performing most signal processing tasks and control other features.

3.3 Universal Software Radio Peripheral

The USRP¹ is an extremely flexible USB device that connects a PC to the RF world. It is a hardware platform that encompasses the software radio paradigm, and has been designed to interface primarily with the GNU Radio software, thus providing a flexible, high speed software radio prototyping test bed. The USRP consists of a motherboard, housing a FPGA for high speed signal processing; ADCs and DACs; and interchangeable daughter boards to cover different frequency ranges [7]. Figure 3.2 below shows the block diagram of the USRP and daughter boards.

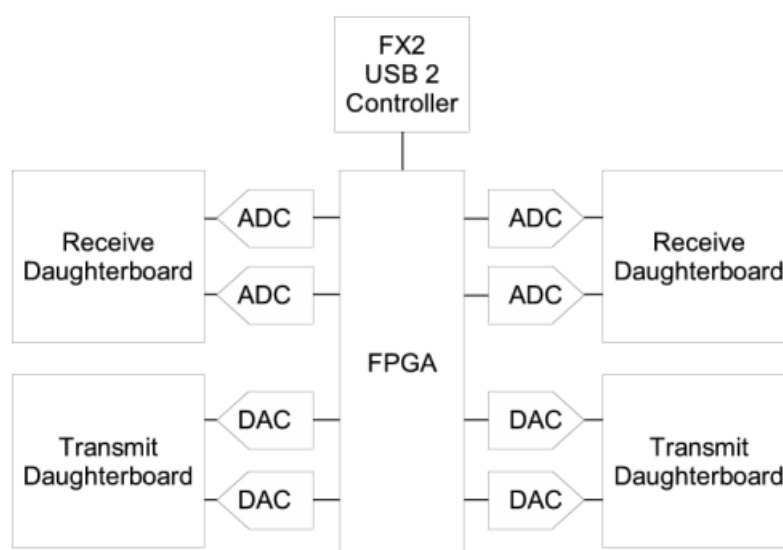


Figure 3.2: Block diagram of USRP and daughter boards [7]

The overall receiver system is illustrated in figure 3.3 below.

3.3.1 FX2 USB 2 Controller

The FX2 microcontroller contains an embedded USB 2.0 transceiver and handles all USB transfers with the upstream USB host. It presents a data bus to the FPGA, with generic control signals which can be programmed to behave in a custom manner. The FX2 also handles all USB control requests, which all USB devices must support to fully comply with the USB standard, including standard setup requests [31].

3.3.2 ADC and DAC

Within the motherboard, it contains up to four 12-bit 64 Msamples/second [7], and with reference to the nyquist criterion, the ADCs are capable of digitizing a band 32MHz wide.

¹Refer to appendix for an image of the USRP and daughter boards.

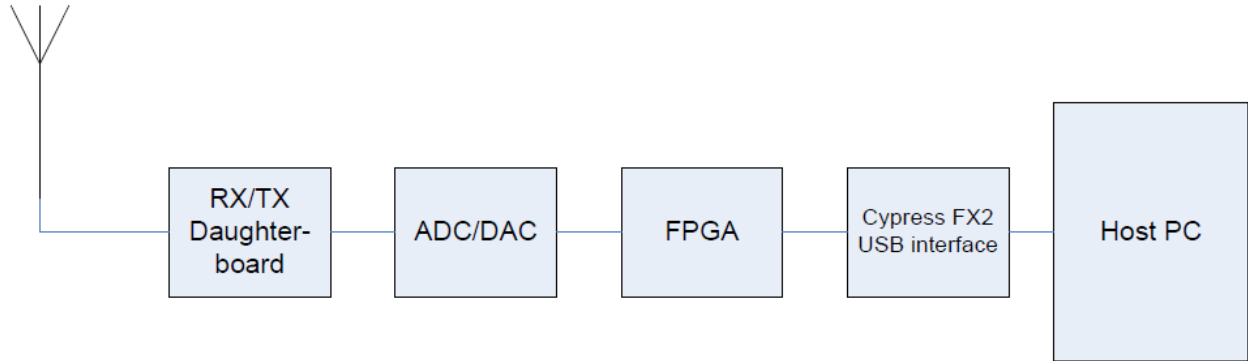


Figure 3.3: Receiver system overview

Positioned ahead of the ADCs there are *programmable gain amplifiers* (PGA) with 20dB of gain available to adjust the input signal level in order to maximise use of the ADCs dynamic range. This approximates to 72dB of dynamic range. The full range on the ADCs is 2V peak to peak, and the input is 50 Ω differential [29].

There are four 14-bit, 128 Msamples/second DACs within the motherboard. The DAC can supply a 50 Ω differential load, with 10dBm. There is also FPGA used after the DAC, providing up to 20dB of gain.

In any digitization process, the faster the signal is sampled, the lower the noise floor, because, although the total integrated noise remains constant, it is now spread out over more frequencies which has benefits if the ADC is followed by a digital filter. Furthermore, the relationship between the SNR and sampling rate in the signal bandwidth is given by:

$$SNR = 6.02N + 1.76\text{dB} + 10\log\left(\frac{f_s}{2B}\right) \quad (3.1)$$

Where:

- N is the number of bits of resolution of the ADC
- f_s is the sampling rate of the ADC
- B is the Bandwidth of the signal

3.3.3 FPGA

There is a million gate FPGA employed in the motherboard. The FPGA used by the USRP is the Altera Cyclone and performs the high speed signal processing. The FPGA also manages the signal including reducing the data rates to facilitate their transport over the USB interface chip to the host PC. The FPGA and the FX2 chip are programmed over the USB2 bus [7]. The clock provided by the USRP drives the ADCs at 64 Msps. This may be divided by two to reduce the sample rate. This only effects the clock rate of the ADCs, as most of the sample rate conversion is done in the FPGA.

After signal digitization, the data is sent to the FPGA. Standard FPGA firmware provides two Digital Down converters (DDC). The DDC allows selection of parts of the digitized spectrums of interest, translate it to baseband and decimate as required. An advantage of performing this function in the digital domain is that the centre frequency can be changed instantaneously, which is useful for frequency hopping spread spectrum systems [7]. The FPGA uses a multiplexer to connect the input stream from each of the ADCs to the inputs of the DDCs. The multiplexer allows the USRP to support both real and complex input signals and allows for having multiple channels selected out of the same ADC sample stream. The DDCs operate as either real down converters using the data from one ADC fed into the real channel, or as complex downconverters where the data from one ADC is fed to the real channel and the data from another ADC is fed to the complex channel via the multiplexer.

The DDC consists of a *numerically controlled oscillator* (NCO), a digital mixer, and a cascaded integrator comb (CIC) filter. These components down convert the desired channel from the IF to baseband, reduce the sample rate and provide low pass filtering. The effects of the NCO and multiplier are implemented using the CORDIC algorithm [7]. This is shown in figure 3.4.

There is a slight difference in the processing steps between the transmit and receive paths. Since the USB bus operates at a maximum rate of 480 Mbps the FPGA must reduce the sample rate in the receive path. The decimator can be treated as a low pass filter by a down sampler. Suppose the decimation factor is M . The low pass filter selects out the band $[-\pi/M, \pi/M]$ from the spectrum, and then the downsampler spreads the spectrum to $[-\pi, \pi]$. Thus the digital signal's bandwidth has been narrowed by a factor of M .

In the transmit path for the USRP it is similar to the receive path, but because the sample rate of the DAC is 128Msps, as opposed to the ADC of 64Msps, it is necessary to increase the sample rate in order to match the sample rates between the high speed data converters and the lower speeds supported by the USB connections. This is done by an interpolater running on the FPGA.

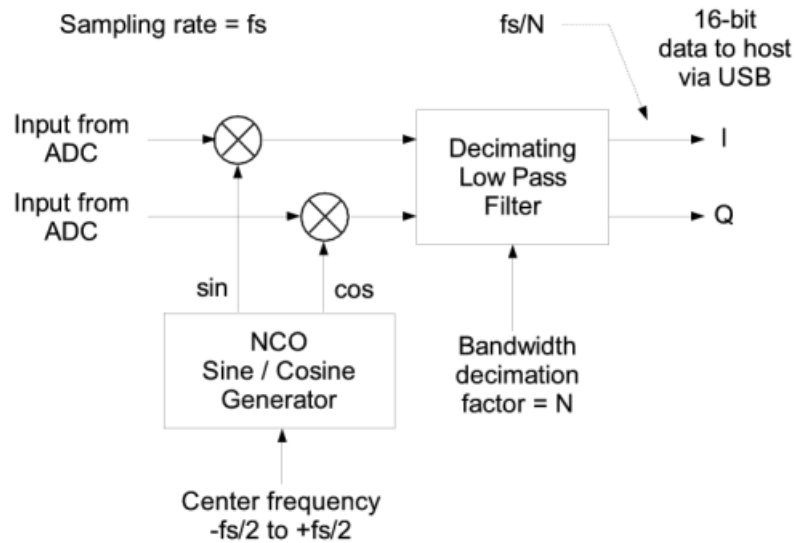


Figure 3.4: DDC block diagram [7]

3.3.4 Daughter Boards

There are four slots on the motherboard, two slots for RX daughter boards, labelled RXA and RXB, and two slots for TX daughter boards, labelled TXA and TXB. The daughter boards are used as the RF receiver interface or tuner and the RF transmitter.

Each of the RX and TX daughter boards has access to two of the four high-speed ADC inputs and DAC outputs respectively. This allows each daughter board which uses real sampling to have two independent RF sections, and two antennas, thus a total of four for the whole system. If complex IQ sampling is used, each board can support a single RF section, for a total of two for the whole system. There are a number of daughter boards available for specific frequency ranges. These includes [11]:

- Basic Tx and Rx Boards
- LFTX and LFRX Boards
- DBSRX
- RFX
- TVRX

All of the daughter boards have their own specific properties including frequency spectrum specific. The TVRX daughter boards will be used as the front end for a PCL system and will be used in all

experimentations conducted. Thus it will form part of the characteristics presented in this thesis.

The TVRX daughter boards is a complete VHF and UHF receiver system based on a TV tuner module. It operates over a 6MHz wide block of spectrum between a range of 50-860MHz. All the tuning functions can be controlled from software.

3.4 GNU Radio

GNU Radio is a free toolkit, open source software platform used for building and developing software defined radio systems. It was started in 1998 and now has a large worldwide community of developers and users that have contributed to a substantial code base and provided many practical applications for the hardware and software [20].

Fundamentally GNU Radio is a signal processing package used to access the electromagnetic spectrum. It provides a complete development environment to create software radios, handling all of the hardware interfacing, multi threading and portability issues. It can act as a stand-alone software package or as a back end to a hardware device [25]. GNU Radio has libraries for all common software radio needs including various modulations, error-correcting codes, signal processing constructs and scheduling. It is a very flexible system and allows applications to be developed in C++ or Python.

3.4.1 Software Architecture

GNU Radio is organised into the following three tier architecture that provides a data flow abstraction [16]:

- Python scripting language used for creating flow graphs
- C++ used for creating signal processing blocks
- Scheduler, used to control the flow graphs

Python scripting is used to build applications for high level organisation, and other non performance critical functions by employing the concept of a graph, containing signal processing blocks and connections for data flow between blocks or “signal flow graphs”.

The signal processing blocks are implemented and correspond to some sophisticated functions or class methods in C++. There is already an existing library of processing blocks within the GNU

Radio framework, including filters, demodulators and other signal manipulation elements. OFDM functionality is currently being added and tested which will be included in the library.

The scheduler uses Python's built-in module threading, to control the 'starting', 'stopping' or 'waiting' operations of the signal flow graph.

A graph can be thought of as a framework upon which all the necessary elements are placed and then connected. Conceptually, blocks process infinite streams of data flowing from their input ports to their output ports. Some blocks have only output ports or input ports. These serve as data sources and sinks in the graph. The signal source can have various implementation, but is usually the USRP or a file containing sampled data. The signal streams then flows through any number of processing nodes. The final output of the processing graph terminates in a signal sink, which may be a real time spectrum analyser, a real time oscilloscope, an output file, The USRP or audio hardware. Figure 3.5 below shows a simple diagram of a flow process.

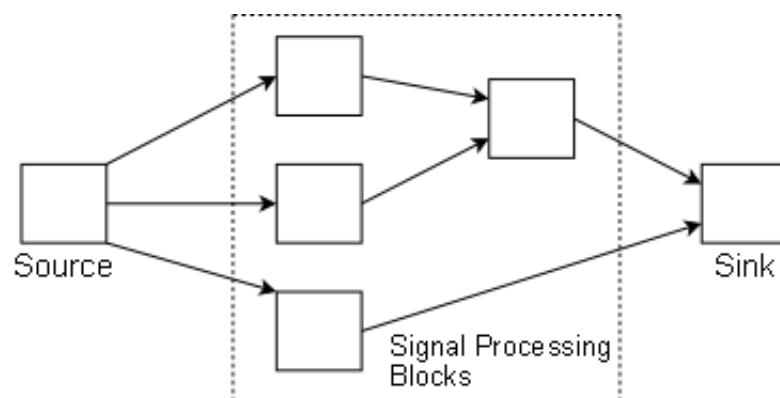


Figure 3.5: Block diagram of flow graph [29]

3.4.2 Hardware

There are various hardware options available for use with GNU Radio. Hardware such as a sound card may be used as an output sink. Wide band I/O and VXI/cPCI cards have suggested as additional option [20]. However the most popular choice of hardware used with GNU Radio is the USRP.

3.5 Summary

Software defined radio is a highly flexible tool used in radio technology, that uses software to define and process signal waveforms. It allows users to easily access the electromagnetic spectrum and deal with radio hardware problems in software. This chapter presents the definitions and concepts

of SDR, including its applications and development tools.

The USRP and GNU Radio is discussed and examined in this chapter. The USRP hosts up to four 12-bit, 64 Msamples/second ADCs and four 14-bit, 128 Msamples/second DACs. The USRP provides a flexible FPGA as its processing unit, which implements a great deal of signal processing in both the receive and transmit chains, including data rate reduction for transportation over the USB interface to the host PC. On the motherboard of the USRP four slots are available for two RX daughter boards and two TX daughter boards. These daughter boards provide front end flexibility allowing for the down conversion of the radio spectrum, and thus manipulation of the spectrum.

GNU Radio is seen as a powerful toolkit that implements numerous signal processing elements, and provides a complete development environment to create software radios, handling all the hardware interfacing. Several hardware interfaces are compatible for use with GNU Radio, with USRP being the most popular. Thus, with the combination of both the USRP and GNU Radio, a powerful and highly flexible tool set for the development of a variety of radio devices is provided.

The following chapters will test the use of the USRP and GNU Radio. It will be used to characterize and simulate the receiver channels of a PCL radar system.

Chapter 4

Oscillator and Frequency Stability

4.1 Introduction

Stability is a measure of how well a frequency source is able to generate a given frequency over some measure of time, once it has been set. Thus the difference between the frequency at one moment in time and another moment is called stability. In Passive radars frequency stability is a limiting factor on its performance because it needs to maintain timing accuracy in order for the precise detection and tracking of targets. Local oscillators are used in the down conversion of frequencies, thus the stability of frequencies is dependent on the performances of the oscillators. The instantaneous frequency generated by any real oscillator circuit changes over time due to both internal and external factors. This chapter introduces some of the oscillator characteristics and will discuss the effects on frequency stability. The local oscillators in the TVRX daughter boards of the USRP is a 4MHz quartz crystal oscillator [29], thus discussions will focus on the properties of the crystal oscillator.

4.2 Quartz Crystal Oscillator

Crystal oscillators are widely used as frequency sources and used in a wide variety of applications. These oscillators provide good performances at a reasonable price and dominate the field of frequency sources. The quartz crystal in the oscillator resonates mechanically and the associated oscillations of the resonator have to be sensed. This is done by taking advantage of the piezoelectric effect. This effect is observed when a physical compression of the crystal generates a voltage across the crystal. Conversely, the application of an external voltage across the crystal causes the crystal to either expand or contract depending on the polarity of the voltage [23].

The resonance frequency and other properties of the quartz crystal oscillator are determined by the size, shape and angle of the cut of the quartz bar or plate, although the limitations in stability are

mainly caused from the noise generated by the electronic components in the oscillator circuitry. These effects can be mitigated using low noise components and optimal circuit design. In addition, the stability depends on many environmental factors, including temperature, time, vibrations and shock etc. The stability is usually given for a number of time periods, ranging between seconds and years [5, 29].

4.2.1 Dependence on Temperature

Temperature is a major influential factor effecting the performances of the oscillator, by changing the elastic properties of the crystal. Temperature affects the density and thickness of the quartz plate, thus affecting its resonance frequency. A direct temperature effect is caused by the temperature dependence of the density of the quartz, and an indirect effect is due to the coefficient of thermal expansion, which changes the thickness of the quartz plate [23].

4.2.2 Long-Term Dependence on Time (Ageing)

The long-term dependence on time or ageing of a quartz crystal oscillator can be defined as the gradual drift of the average frequency. Drift is due to ageing plus changes in the environment and other external factors. Ageing, on the other hand, is defined as the systematic change in frequency due to physical changes in the oscillator. These physical effects include [23]:

- Temperature gradients
- Stress relief
- Change of mass
- Structural changes

Temperature gradients may last from several minutes to several hours after thermal disturbances. Stress relief depends on the previous thermal history and can last from three days to three months. The change of mass are caused by a gain or loss of mass on the crystal surface lasting up to a period of several weeks to several years. Structural changes are effected by impurities in the crystal lattice. These ageing rates decreases with time. Quartz crystal oscillators age either up or down and will not change their ageing pattern.

4.2.3 Short-Term Dependence on Time

Superimposed on the gradual drift are short-term fluctuations. Fluctuations of the frequency about the average frequency are caused by absorption and desorption of gases by the crystal as well as

the stresses between the quartz and its electrodes. Stresses are due to vibrations and accelerations, which affects the loading on the quartz plate. Vibrations do not cause major failures of the unit, but rather causes shifts in the frequency and changes in the resistance [23].

4.2.4 Types of Crystal Oscillators

As mentioned before temperature is by far the largest source of error in oscillator units. Thus, the large demand for more precise oscillators has led to the development of specialized oscillators exhibiting greatly reduce sensitivity to changes in ambient temperature. These include [5, 23]:

- Room Temperature Crystal Oscillator (RTXO)
- Temperature Control Crystal Oscillator (TCXO)
- Oven Control Crystal Oscillator (OCXO)

RTXO operates at ambient temperature and incorporates a quartz crystal resonator of minimum change in frequency over a large temperature range.

TCXO incorporates sable thermistors that compensate for the temperature drift of the oscillator. The temperature characteristics of a TXCO is typically five times than that of a RXCO.

OCXO employ a controlled environment for the quartz crystal and possibly for the entire oscillator circuitry, by operating at an elevated temperature above the highest temperature to which the instrument is likely to be exposed.

4.2.5 Performance of Quartz Crystal Oscillators

The performances of the quartz crystal oscillators is mainly determined by the frequency stability of the quartz crystal resonator, although other factors such as circuitry also contribute to the performances. The most important stability parameter is the temperature. To compensate for temperature, different types of oscillators have been developed and was discussed in section 4.2.4.

Long-Term Stability Performances

This gradual drift of the average frequency is caused by the ageing of components, notably the quartz crystal. The long term stability is specified for a certain time interval, namely years, months or days, depending on the oscillator. RTXOs and TCXOs cannot be specified in terms of days because effects caused by small temperature variations are too large to allow the measurement of the long-term drift in such a short time. Ageing rates of OCXO are measured after the initial warm-up period and are based on continuous operation and sometimes optimum environment. Typical ageing rates are shown in table 4.1 below [23]:

Oscillator types	per day	per month	per year
RTXO	-	3×10^{-7}	3×10^{-6}
TCXO	-	1×10^{-7}	1×10^{-6}
OCXO	5×10^{-10}	1.5×10^{-8}	2×10^{-7}

Table 4.1: Typical ageing rates (Long-term)

Short-Term Stability Performance

Short-term stability is defined as the frequency fluctuations for a specific average time. Useful counting intervals range from $1ms$ to $100s$. The short term stability improves with an increase in the length of the counting interval. Short-term fluctuations are caused by thermal and shot noise perturbing the oscillations. Additional short-term fluctuations may be caused by interference from sources outside the oscillator circuit. Typical short-term stability specification are listed in table below [23]:

Oscillator Types	Short-term stability (1s average)
RTXO	2×10^{-9}
TCXO	1×10^{-9}
OCXO	5×10^{-10}

Table 4.2: Typical short-term stability rates

4.2.6 Warm-Up Effect

The warm-up effect is caused by the rise in temperature from the time the oscillator and instruments is turned on to the time a stable operating temperature is reached. Therefore the warm-up effect is also a time effect. The temperature rise is brought about directly by power dissipation in the oscillator or indirectly by the generation of heat of the circuitry of the entire instrument.

4.3 System Setup

This section will describe the experimental setup and overview of the system used for testing. The test signal is generated by a Hewlett Packard 8656B signal generator. The signal was tested at two separate frequencies of 89MHz and 100MHz. This signal is split and sent to the USRP with two TVRX daughter board modules, running simultaneously. This will model the PCL receiver with independent TVRX modules for the reference channel and the target return channel. The microtune TVRX daughter board can handle a maximum input signal level of $80dB\mu V$. This translates to a maximum input voltage of $10mV$, thus a maximum input power of $-8.75dBm$ ¹. The signal generator

¹The daughter boards have a 75Ω differential input, thus power is $\frac{10mV}{75\Omega} = 0.133mW$ ($-8.75dBm$).

will be set to a power level of -10dBm. Independent signals are then digitized by the USRP. ADCs are clocked by the same master clock running the USRP, thus synchronization between ADCs are ensured. Figure 4.1 below shows the functional block diagram of the setup used in the following experimentations².

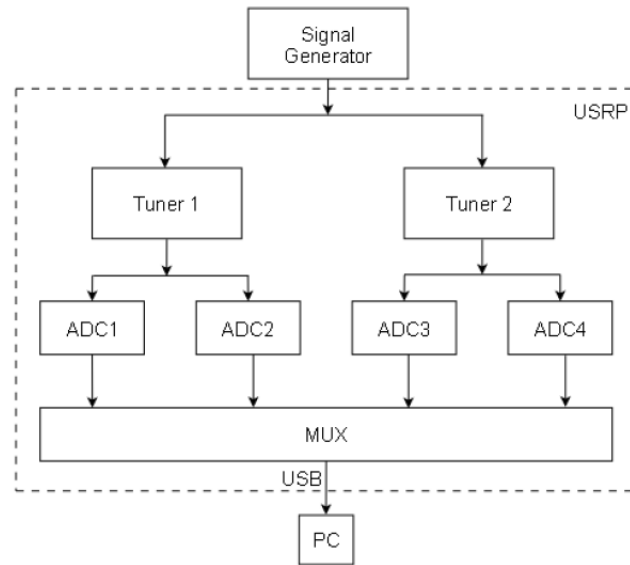


Figure 4.1: Block diagram of experimental setup

GNU Radio was configured such that the signals from TVRX 1 and TVRX 2 are written to separate files on the PC, which is then used for post processing. The experiment was conducted with a maximum decimation rate of 256. With the ADCs maximum sampling rate of 64 Msamples/second, and using 256 decimation rate, this translates to a sampling frequency of 250kHz on the ADC. The system was setup to determine the oscillator stability over thirty minute periods, and thereafter one hour periods. This was achieved by taking successive readings of the frequency output by each tuner over the thirty minute period, and each reading was obtained by averaging the output frequency for one second time gate, every minute for thirty minutes. The resolution of the measured frequency is given by:

$$\Delta f = \frac{1}{T} \quad (4.1)$$

Where T is the time gate over which the frequency is averaged.

²Refer to appendix to view photograph of equipment.

4.3.1 Results

This section will show some of the results obtained from the experimentations. For consistency, images shown are those of the 100MHz signal. The daughter boards has been tuned accordingly with USRP decimation rate of 256. Signals are then down converted to 10kHz.

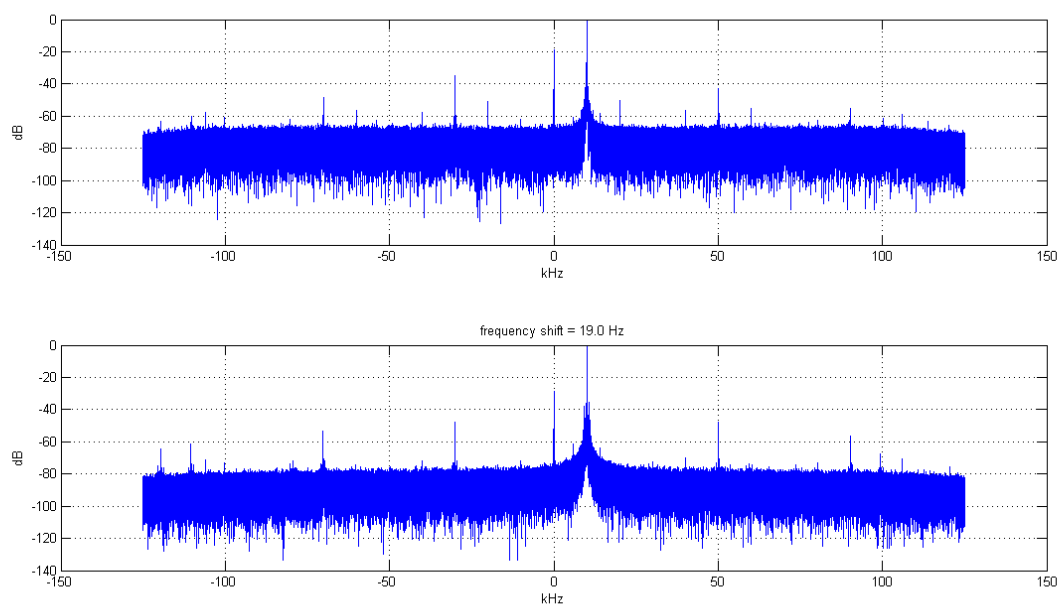


Figure 4.2: Frequency positions at start of the experiment

Figure 4.2 shows the positions of the peaks of the centre frequency between the two channels as well as the relative shift between the two. A closer look at the peak during the start time is shown in figure 4.3.

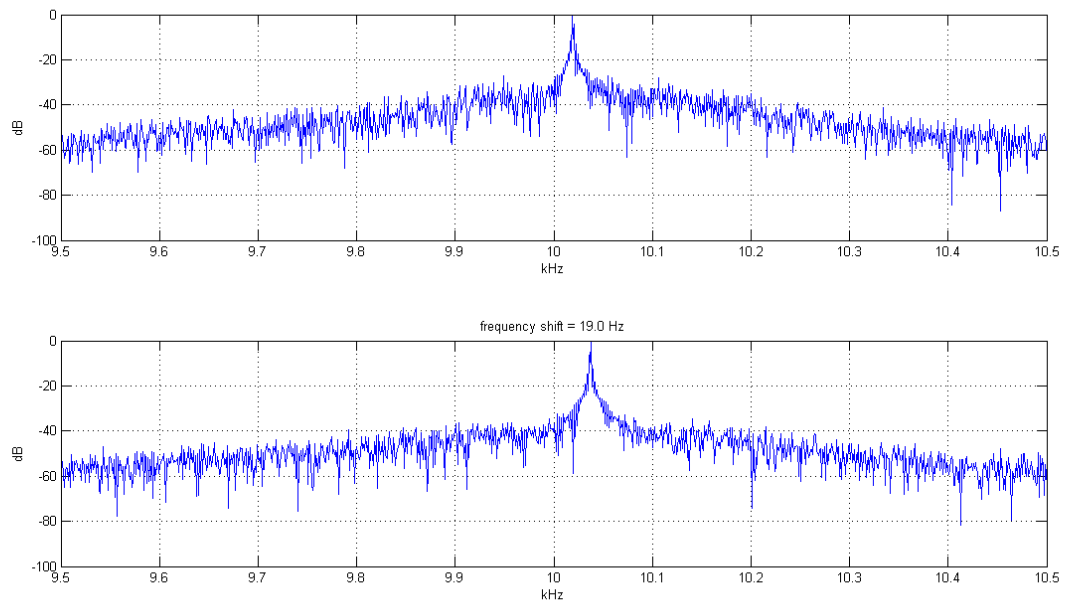


Figure 4.3: Frequency positions at start of experiment (zoomed)

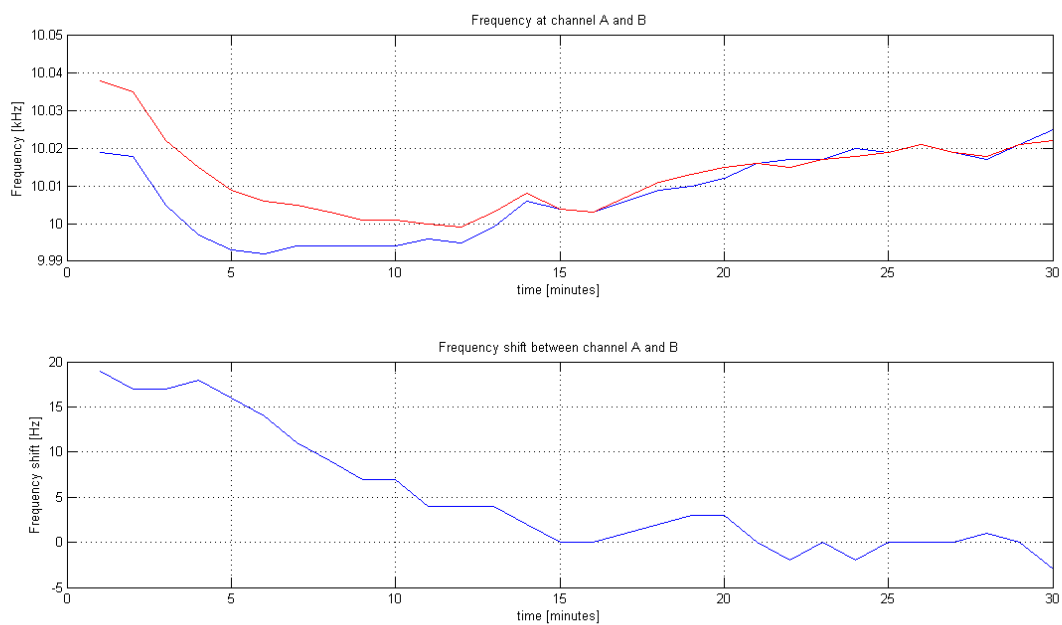


Figure 4.4: Frequency drift of both channels and relative frequency shift

Figure 4.4 shows the drift between the channels over the thirty minute period as well as the relative frequency shift between the two channels. It can be seen that there is a frequency offset between the two channels at the start of the experiment. This offset or shift gradually reduces over time. This

may be seen as the warm-up effect described in section 4.2.6, as the frequency gradually stabilizes over time.

Measurements of thirty minute periods are taken repeatedly with approximately one hour between each measurement. Thereafter, one hour measurements are taken to see the response and performances of the USRP and daughter boards. This process was done over several days, to measure the drift over longer periods of time.

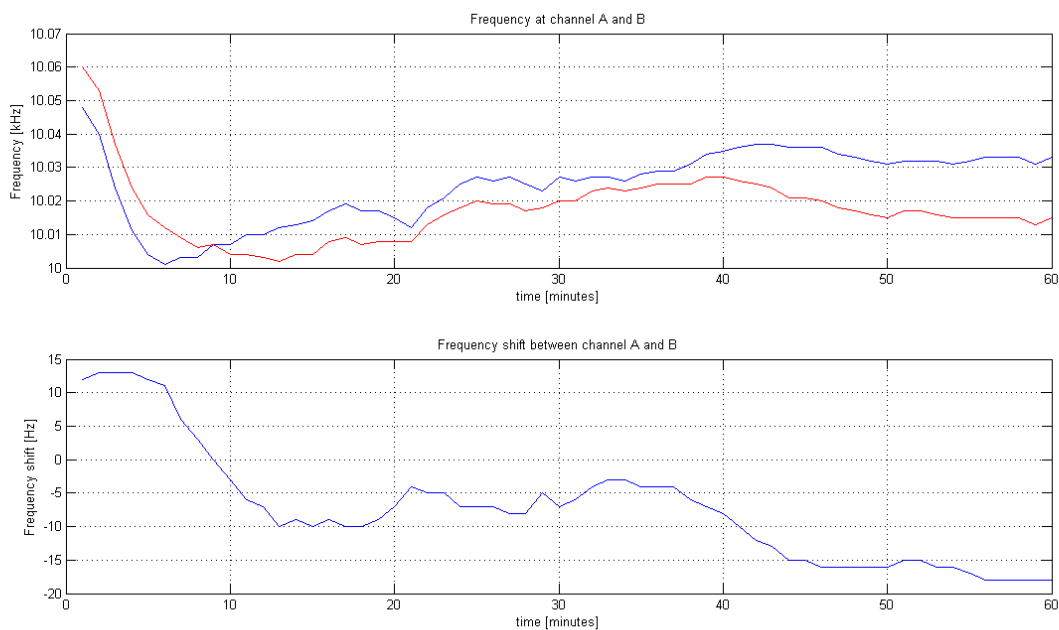


Figure 4.5: Frequency drifts of both channels and relative frequency shift over one hour

From figure 4.5 and results obtained after the measurements, it was seen that the results were inconsistent. It was determined that this inconsistency is mainly due to the fact that, between the one second time gate periods of sampling as well as the periods in between 30 minute/1 hour measurements, the USRP was off, thus ADC conversion had stopped between these periods. As a result, ADCs were converting inconsistently, thus the effects of oscillator and frequency drifts was not accurately modelled.

To improve the modelling process, the signal was sampled and converted continuously over one minute. Post processing of the signals that were sampled for several minutes was not possible due to the large amounts of data from continuous sampling. By using the maximum decimation rate of 256, ADCs sample at 250kHz, thus 15 millions samples are made in one minute, amounting to 120MB of data.

Figure 4.6 shows the relative drift of both channels over one minute. Over one minute the drift is

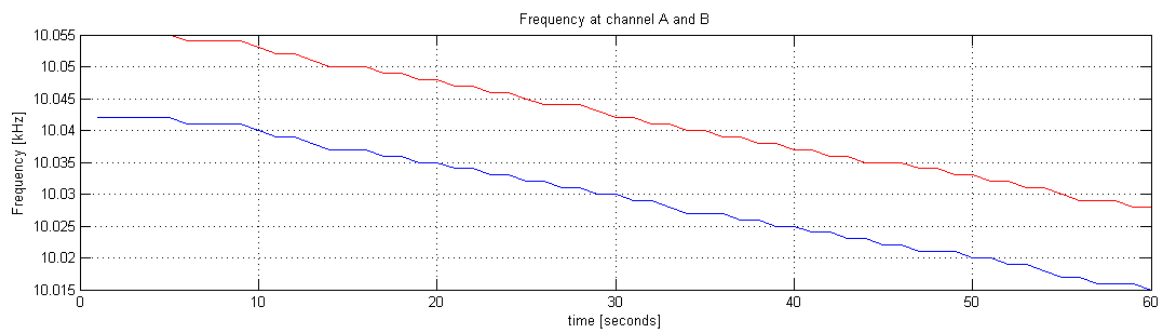


Figure 4.6: Frequency drifts of both channels over 1 minute

more stable and consistent, and it can be seen that there is still a frequency offset between the two channels. This offset can be seen on figure 4.7 below.

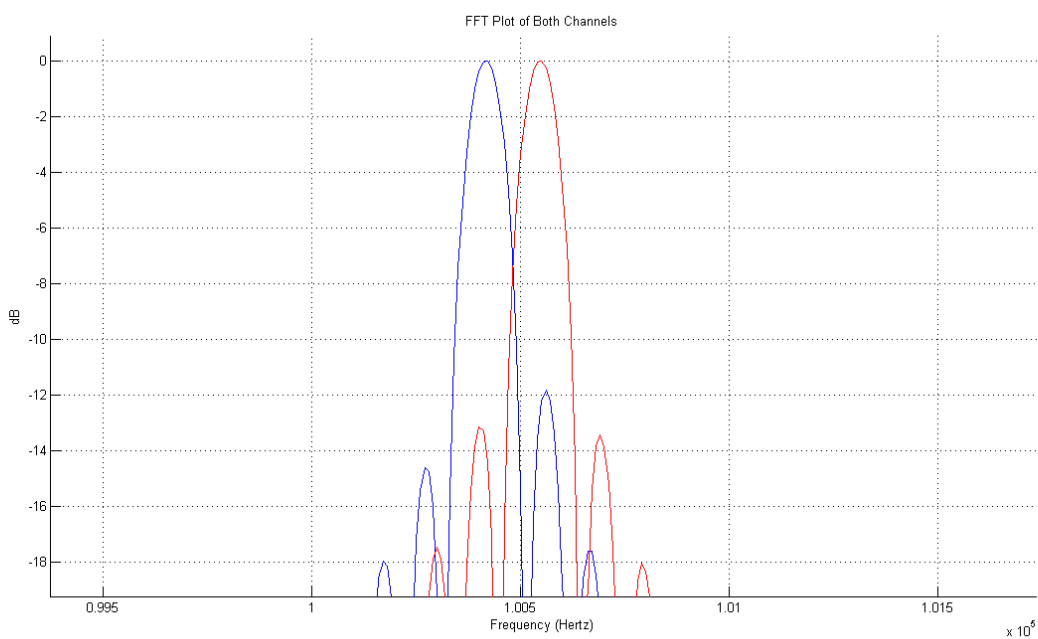


Figure 4.7: Offset between channels

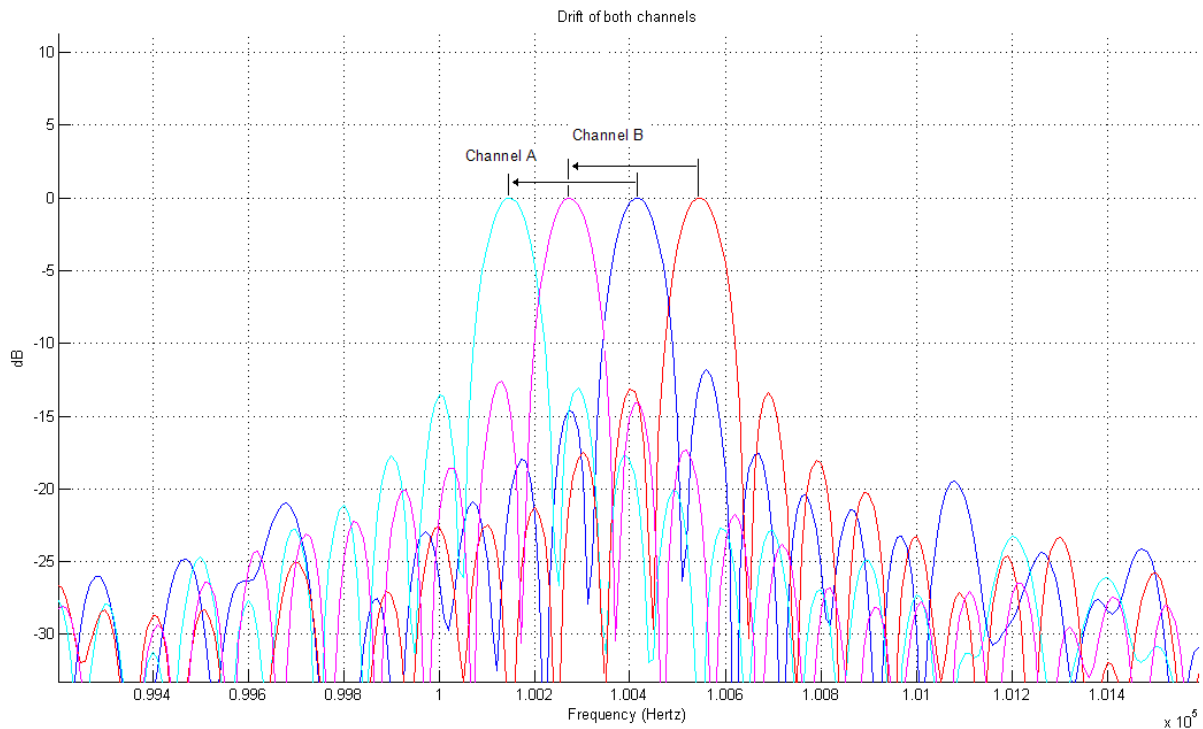


Figure 4.8: Position of peaks over one minute

Figure 4.8 demonstrates the drift of both channels over one minute. This can be used to model and estimate the drift over longer periods of time. The peaks of the FFT of the signals shows the position of the frequency, due to its resolution these peaks may have small errors in its position, thus to model the drift it is necessary to investigate the phase of the signals. This will be done in the next chapter.

4.4 Summary

This chapter shows that the performances of radar applications are limited to the ability of the radar's frequency to maintain timing accuracy and frequency stability. This ability is limited by the performances of the local oscillators within the radar.

The local oscillators in the TVRX daughter boards of the USRP is a 4MHz quartz crystal oscillator. Thus, the properties of crystal oscillators and the associated performance parameters of interest were investigated. These parameters included its dependence on temperature, ageing and short term effects.

Experimentation was done with the USRP and TVRX daughter boards to measure the stability and the relative drifts between two channels with the same input signal. This is used as a model for PCL



receivers. The results will be further investigated in chapter 5 and will be used to characterize the drift and stability of these signals by presenting the relationship between frequency and phase.

Chapter 5

Frequency Drift Characterization

5.1 Introduction

In order to model the performances of the oscillator, random and deterministic variations in time and frequency needs to be characterized. In this chapter techniques associated with time and frequency characterization will be presented as well as investigating the relationship between frequency and phase.

Linear drifts in frequency is an important element in most models of oscillator performances. Quartz crystal oscillators often have drifts in excess of 1 part in 10^{10} per day. Even highly stable devices such as cesium beams show drifts of a few parts in 10^{13} per year. There are several ways to estimate the drift rates from data samples such as regress phase to a quadratic; regress frequency to a linear; compute simple mean of the first difference of frequency; use Kalman filters with a drift element in the state vector; and others [6]. Although most of these estimators are unbiased, they vary in efficiency or confidence intervals. These estimators, using standard analysis of variance can give optimistic results.

5.2 Frequency Domain Characterization

It is assumed that the average output frequency of a precision oscillator is determined by a narrow band circuit, so that the signal can be approximated as a sine wave [1], and thus generalized by this formula:

$$V(t) = [V_0 + \varepsilon(t)] \sin \Phi(t) \quad (5.1)$$

Where:

- V_0 is the nominal peak voltage
 $\varepsilon(t)$ is the deviation of the amplitude from nominal
 $\Phi(t)$ is the total oscillator phase

This can be rewritten, as the $\varepsilon(t)$ in precision oscillators is generally ignored and placing all of the deviations in a residual phase:

$$V(t) = V_0 \sin[2\pi\nu_0 t + \phi(t)] \quad (5.2)$$

Where:

- $\phi(t)$ is the deviation of the phase from the nominal

By defining the fractional or normalized frequency deviation of $\nu(t)$ from its nominal value as:

$$y(t) = \frac{\nu(t) - \nu_0}{\nu_0} \quad (5.3)$$

Which is dimensionless, and by integrating $y(t)$, will yield the time deviation $x(t)$.

$$x(t) = \int_0^t y(t) dt \quad (5.4)$$

From equation 5.4, the time deviation of a clock can be written as a function of the phase deviation:

$$x(t) = \frac{\phi(t)}{2\pi\nu_0} \quad (5.5)$$

5.2.1 Drift Characterization

Almost all oscillators display a superposition of random and deterministic variations in frequency and phase. This includes, frequency drifts, frequency offsets, time offsets as well as environmentally induced systematic deviations. The most typical model used to characterize these variations is [6]:

$$x(t) = a + bt + \frac{D_r}{2}t^2 + \varepsilon(t) \quad (5.6)$$

Where:

- $x(t)$ is the time (phase) error of the oscillator
 a is the initial time offset
 b is the initial frequency offset
 Dr is the frequency drifts
 $\varepsilon(t)$ is the random deviations

$x(t)$ is a random variable by virtue of its dependence on $\varepsilon(t)$. Even though one cannot predict future values of $x(t)$ exactly, there are often significant auto-correlations within the random parts of the model. These correlations allow forecasts which can significantly reduce clock errors. Errors in each element of equation 5.6 contribute their own uncertainties to the predictions and are dependent on the time of the forecast interval.

A notable point from equation 5.6 is that the linear drift term in the model will eventually overcome all other uncertainties for a sufficiently long forecast interval. While it is possible to measure the drift coefficient, Dr , and make corrections, there will always be some uncertainty in the value used.

5.2.2 Relative Drift of Two Channels

To measure the relative frequency drifts between two receiver channels, the use of the USRP is once again used with two TVRX daughter boards. Within the daughter boards are free running oscillator clocks, LO_1 and LO_2 . Both of these oscillators are compared to a stable reference clock, which is set to a frequency of 100MHz. The measurement is done by means local oscillators within the mixers of the daughter boards. Two signals are generated independent of each other and correspond to the frequency difference, and sum between the local oscillators and the reference clock. After low-pass filtering and digitization through the ADCs, and digitally down converted, both signals $s_1(t)$ and $s_2(t)$ have an initial frequency of 10 kHz. These signals correspond to:

$$s_1(t) = S_1 e^{j\varphi_1(t)} \quad (5.7)$$

$$s_2(t) = S_2 e^{j\varphi_2(t)} \quad (5.8)$$

Where:

- S_1 and S_2 are the respective amplitudes
 $\varphi_1(t)$ and $\varphi_2(t)$ are the instantaneous phases

The measure the relative frequency drift between the two signals equation 5.7 and 5.8 can be rewritten with the initial frequency f_0 . Note that $f_0 = 10\text{kHz}$.

$$s_1(t) = S_1 e^{2j\pi f_0 t + j\phi_1(t)} \quad (5.9)$$

$$s_2(t) = S_2 e^{2j\pi f_0 t + j\phi_2(t)} \quad (5.10)$$

Where:

$\phi_1(t)$ and $\phi_2(t)$ are the residual phases of the oscillator compared to the reference clock

$\phi_1(t)$ and $\phi_2(t)$ can be written as:

$$\phi_1(t) = \varphi_1(t) - 2\pi f_0 t \quad (5.11)$$

$$\phi_2(t) = \varphi_2(t) - 2\pi f_0 t \quad (5.12)$$

Characterization of drift through time deviation

From the model of equation 5.6, it can be seen that the linear and quadratic variations of the residual phase $\phi(t)$ generates a frequency offset (linear variations of the residual phase) and a frequency drift (quadratic of the residual phase), that can be measured. The frequency drift can be characterized accurately by measuring long term variations of the instantaneous frequency but due to the large amounts of data sampled, as was mentioned in chapter 4 measurements of long term basis (several minutes or hours) will be difficult to perform. Instead we can use the linear property of the frequency drift relative to the time, and the fact that we can access the instantaneous phase, φ_1 and φ_2 , of both signals to characterize it on shorter time basis (several seconds). Consequently, it is not possible to compare the frequency variations, by looking at the FFT plots of both signals due to insufficient resolution, therefore the method used consists of measuring the phase errors relative to the time.

The time deviation of both oscillators, compared to the reference clock is defined as the residual phase divided by the initial frequency:

$$x_1(t) = \frac{\phi_1(t)}{2\pi f_0} = \frac{\varphi_1(t) - 2\pi f_0 t}{2\pi f_0} \quad (5.13)$$

$$x_2(t) = \frac{\phi_2(t)}{2\pi f_0} = \frac{\varphi_2(t) - 2\pi f_0 t}{2\pi f_0} \quad (5.14)$$

From equation 5.6 and by letting $c = \frac{Dr}{2}$:

$$x_1(t) = a_1 + b_1t + c_1t^2 + \varepsilon_1(t) \quad (5.15)$$

$$x_2(t) = a_2 + b_2t + c_2t^2 + \varepsilon_2(t) \quad (5.16)$$

To find the relative frequency drift between the two signals, the quantity to characterize is thus $\delta c = c_2 - c_1$. To obtain δc the following methods are used and tested:

- Least square method
- Derivation of the instantaneous phase

Both methods should correspond to the same results.

Least square method

From the instantaneous phases, $\varphi_1(t)$ and $\varphi_2(t)$, we can calculate the time deviation difference between both signals:

$$x_2(t) - x_1(t) = \frac{\varphi_2(t) - \varphi_1(t)}{2\pi f_0} = a_2 - a_1 + (b_2 - b_1)t + (c_2 - c_1)t^2 + \varepsilon_2(t) - \varepsilon_1(t) \quad (5.17)$$

Instantaneous phases are sampled in time, ensuring that the phase variation between two samples is not bigger than 2π (i.e. Nyquist theorem must be respected).

Neglecting the noise terms $\varepsilon_1(t)$ and $\varepsilon_2(t)$, we obtain the following matrix formulation:

$$\delta \mathbf{X} = \mathbf{X}_2 - \mathbf{X}_1 = a_2 - a_1 + (b_2 - b_1)\mathbf{T} + \frac{c_2 - c_1}{2}\mathbf{T} \times \mathbf{I} \times \mathbf{T}^T \quad (5.18)$$

Where:

- \mathbf{X}_1 and \mathbf{X}_2 are the 1-column arrays obtained from the instantaneous phases
- \mathbf{T} is the 1-column array of the corresponding sampling times
- \mathbf{I} is the identity matrix (1 in diagonal, 0 elsewhere)
- \mathbf{T}^T is the transposed (1-line) array of \mathbf{T}

There are more equations in the system than unknown variables and the polynomial coefficients $a_2 - a_1$, $b_2 - b_1$ and $c_2 - c_1$ can be obtained by mean of a least square method. To implement this, the function **polyfit** is used from Matlab, which finds the coefficients of a second order polynomial.

Derivation of the instantaneous phase

From equation 5.17, it can be noted that:

$$\frac{d^2\varphi_2}{dt^2} - \frac{d^2\varphi_1}{dt^2} = 2\pi f_0(c_2 - c_1) + \varepsilon_2(t) - \varepsilon_1(t) \quad (5.19)$$

And once again by neglecting $\varepsilon(t)$:

$$\begin{aligned} c_2 - c_1 &= \frac{1}{2\pi f_0} \left(\frac{d^2\varphi_2}{dt^2} - \frac{d^2\varphi_1}{dt^2} \right) \\ &= \frac{1}{2\pi f_0} \frac{d^2(\varphi_2 - \varphi_1)}{dt^2} \end{aligned} \quad (5.20)$$

The second time derivative can also be implemented in Matlab with the function **diff**, applying it twice to get the results.

5.2.3 State of Oscillators Over Long Periods

Since the oscillator frequency drifts are linear in time and characterized by the coefficients c_1 and c_2 , the frequency may be predicted using the elements of equation 5.6. The relationship between frequency and phase may be given by:

$$\frac{d\varphi}{dt} = 2\pi f(t) \quad (5.21)$$

and the derivative of equation 5.11 is given by:

$$\frac{d\phi}{dt} = \frac{d\varphi}{dt} - 2\pi f_0 \quad (5.22)$$

thus,

$$\frac{d\phi}{dt} = 2\pi f(t) - 2\pi f_0 \quad (5.23)$$

From equation 5.13 and 5.15, and neglecting $\varepsilon(t)$:

$$\phi(t) = 2\pi f_0[a + bt + ct^2] \quad (5.24)$$

thus by relating equation 5.23 and 5.24:

$$\frac{d\phi}{dt} = 2\pi f_0[b + 2ct] = 2\pi[f(t) - f_0] \quad (5.25)$$

From this the frequency may be predicted over a known time by:

$$f(t) = f_0[b + 2ct + 1] \quad (5.26)$$

Note that f_0 is the reference frequency (10kHz in this case), b is the frequency offset coefficient and that c is related to the drift coefficient by $\frac{Dr}{2}$. Equation 5.26 can be used to predict the frequency at later times. This method may also be used to roughly calculate the frequency offset and frequency drift coefficients. This is done by substituting the initial instantaneous frequency at the beginning of the measurements, to calculate the b coefficient. This can then be used to calculate the drift coefficient c by substituting the instantaneous frequency at a known period later in time.

5.3 Time Domain Characterization

In order to determine the stability of the oscillators it is necessary to measure its deviation from its norm. It is inadequate to use the standard deviation σ^2 to measure these variances due to the fact that the instantaneous frequency $y(t)$ and phase $x(t)$ functions are unbounded. Thus, a method called the Allan Variance is used [1]. Allan variance is also known as the two-sample variance and is defined as one half of the time average of the squares of the differences between successive readings of the frequency deviation sampled over the sampling period. The Allan variance depends on the time period used between samples. Therefore it is a function of the sample period as well as the distribution being measured and is displayed as a graph rather than a single number. A low Allan variance is a characteristic of a clock with good stability over the measure period. In discrete sampled systems, the Allan variance is defined as the dimensionless number [2]:

$$\sigma_y^2(\tau) = \lim_{N \rightarrow \infty} \frac{1}{N} \sum_{n=1}^N \frac{(x_n - 2x_{n-1} + x_{n-2})^2}{2\tau^2} \quad (5.27)$$

Where:

- x_n is equivalent to $x(n\tau_0)$
- τ_0 is the system sample rate

$x(t)$ and $y(t)$ are given in equations 5.5 and 5.4 respectively. With only a finite number of data points are available, the Allan variance can be estimated as [2]:

$$\sigma_y^2(\tau) = \frac{1}{N-2m} \sum_{n=1}^{N-2} \frac{(x_{n+2m} - 2x_{n+m} + x_n)^2}{2m^2\tau_0^2} \quad (5.28)$$

Where $\tau = m\tau_0$, τ_0 is the system sample rate, and N data points are available. In band limited systems, the Allan variance is known to converge for all $\alpha > -3$. The Allan variance is useful for characterization of noise as $\sigma_y^2(\tau) \sim \tau^{-\alpha-1}$ for $-3 < \alpha \leq 1$. Thus the Allan variance can be used

to estimate both the intensity and power spectral density of noise. These noise power densities are generalized into the following five power-laws [2]:

- White phase modulation
- Flicker phase modulation
- White frequency modulation
- Flicker frequency modulation
- Random walk frequency modulation

These are shown in figure 5.1 below.

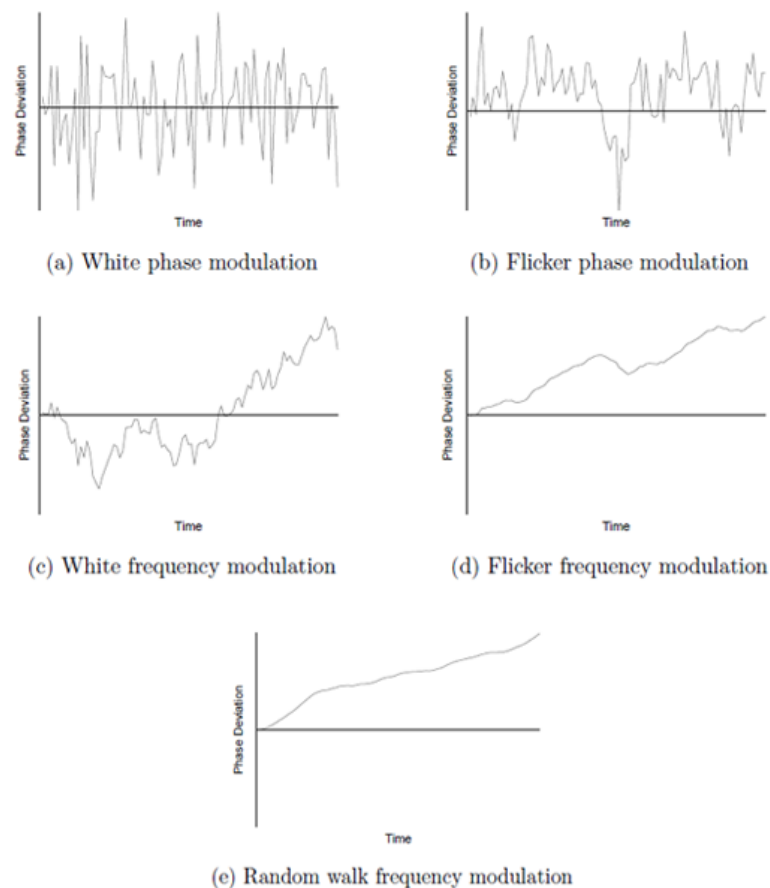


Figure 5.1: Categories of phase noise corresponding to power law spectra [9]

The characterization power of the Allan variance is limited by an ambiguity where $\alpha \geq 1$. It cannot differentiate between white phase modulation and flicker phase modulation noise. This limitation is addressed by the modified Allan variance. Due to the short recording periods of the experimentations these phase noise will not be present thus the modified Allan variance will not be presented.

5.4 Results

The system setup is the same as section 4.3 with one adjustment. The signal generator is replaced with a quartz GPS discipline oscillator (GPSDO), designed by J.S. Sandenbergh [14]. The GPSDO employs a low-cost single carrier GPS receiver and a moderate stability single-oven OCXO. This is a highly stable device with a reasonable price performance ratio and is explain in greater detail in [14]. This device generates a frequency of 100MHz, and is used for its stability in these experiments.

In order to characterize the frequency as well as the drift accurately it is necessary to investigate the phase. The following results will mainly focus on the phase and models of these, thus predictions can be made to determine the drifts over longer periods of time.

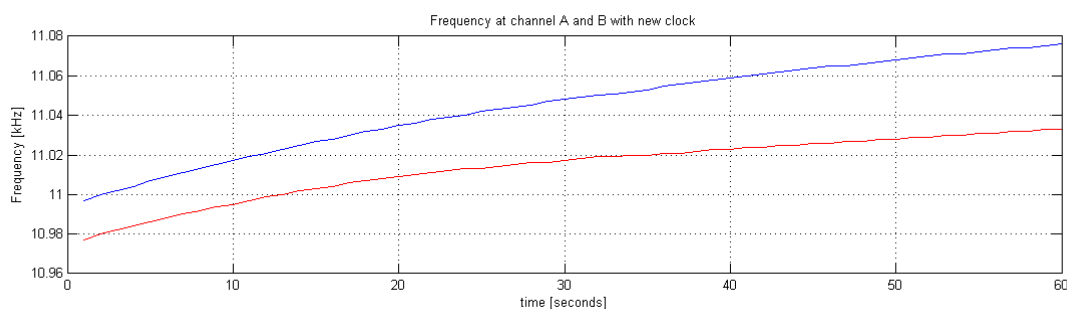


Figure 5.2: Frequency of both channels (Start up)

Figure 5.2 shows the frequency drifts between the two channels. This measurement was taken soon after start up of the equipment.

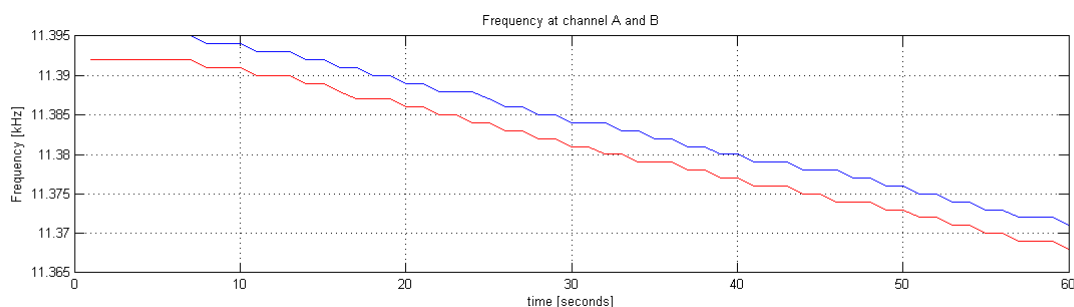


Figure 5.3: Frequency of both channels (Stable conditions)

Figure 5.3 also shows the frequency drift of both channels. This measurement was taken approximately one hour after that of figure 5.2. By comparing figure 5.2 with 5.3, it is clear that the warm-up effect, discussed in section 4.2.6, is present and effects the stability of the system during start up.

To see the relative effects, and thus to regress the phase to a quadratic so to model the signal, the phase is looked at.

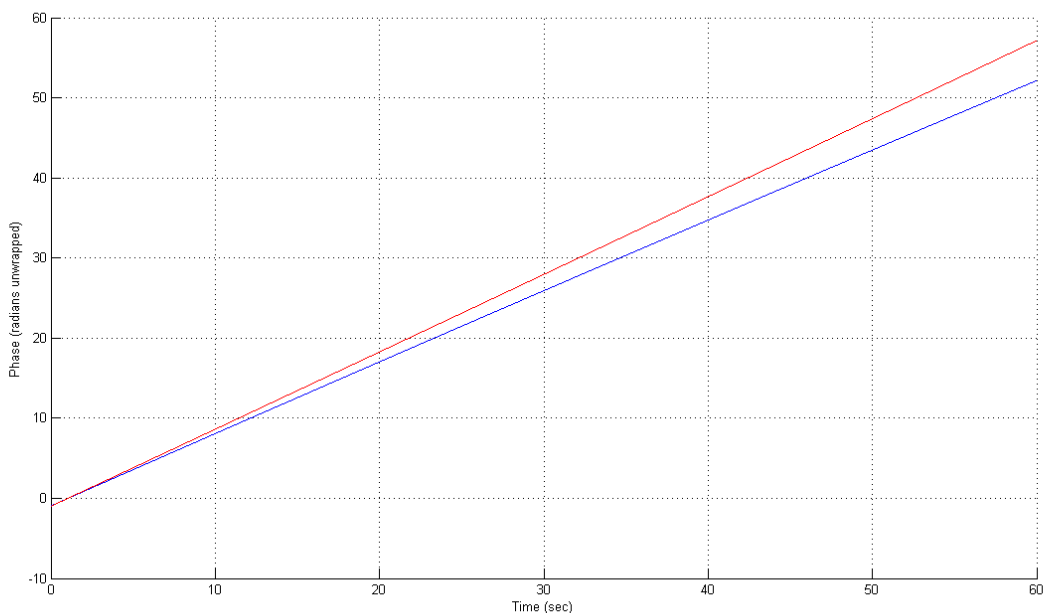


Figure 5.4: Phase of frequencies of figure 5.2

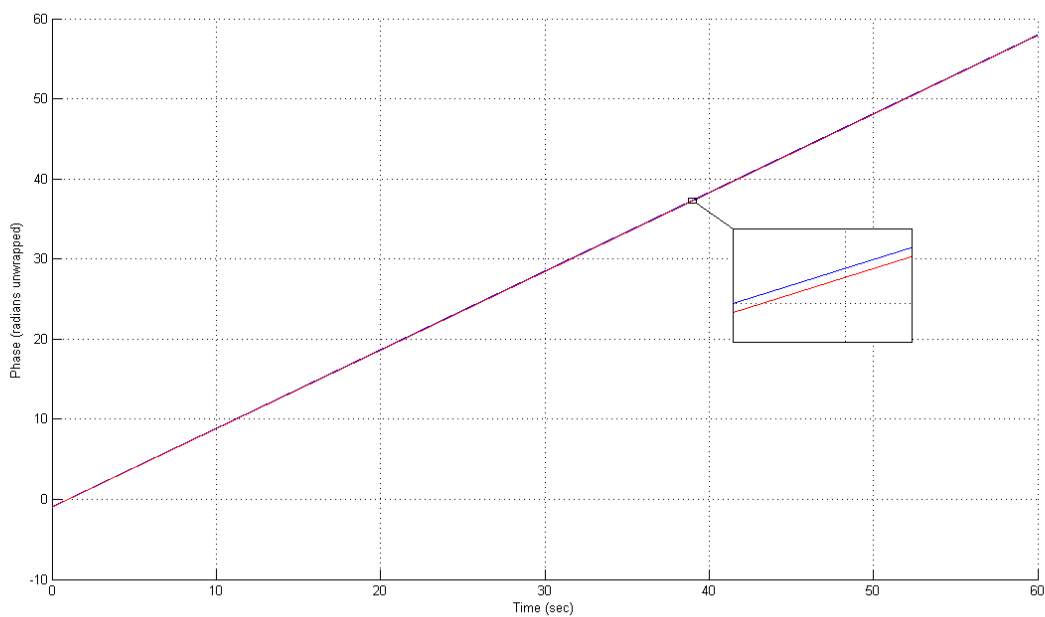


Figure 5.5: Phase of frequencies of figure 5.3

From figure 5.4 it can be seen that the phase during start up drifts apart fairly rapidly. In figure 5.5,

the phase is much more stable and is relatively the same between the two channels.

By using figure 5.5, and the methods discussed in section 5.2.2, the phase can be modelled, thus finding the coefficients of time offset (a), frequency offset (b) and the frequency drift coefficient (D_r). Both methods, discussed in section 5.2.2 was used, and gave the same results. Both channels are modelled and plotted against the actual phase for comparison, where $a + bt + \frac{D_r}{2}t^2$ represents the model (in blue) and is compared to $\frac{\phi(t)}{2\pi f_0}$ (in red).

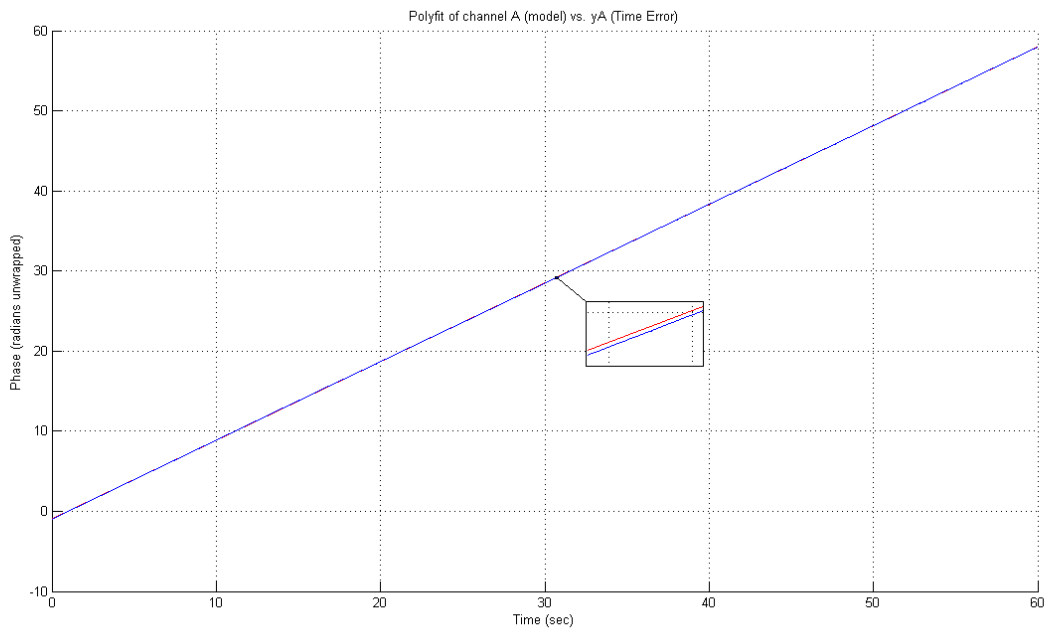


Figure 5.6: Phase model of channel A

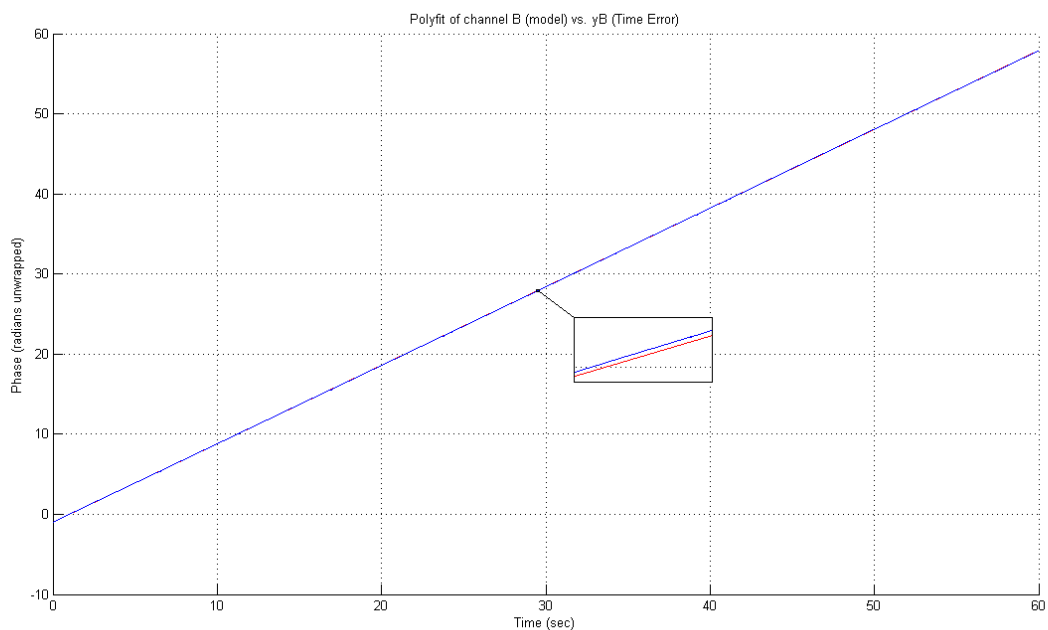


Figure 5.7: Phase model of Channel B

Another method to determine the coefficients is to measure the peak of the FFT, shown in figure 5.8 below, of the frequencies and then use the information to derive the coefficients. This was tested, and results had some correspondence with the previous results, but it is not recommended to use this method as the results are not accurate due to the resolution of the FFTs.

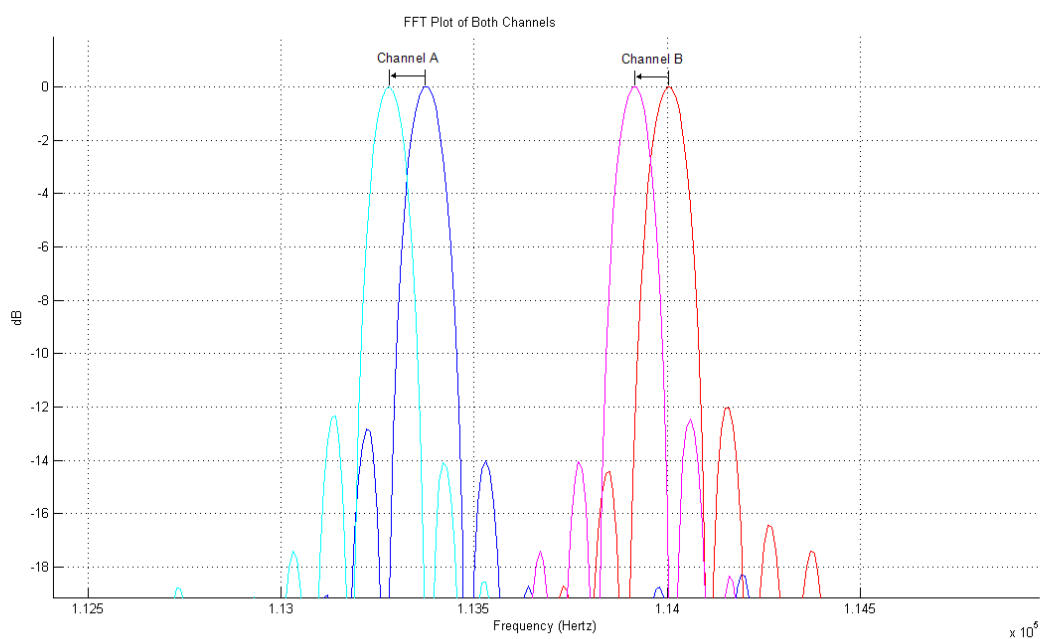


Figure 5.8: Drift in peak of FFT

Although each channel is drifting, the relative drift between the channels is more important, because the two signals will cross-correlated to determine a target's properties. Thus, the relative drift is also modelled.

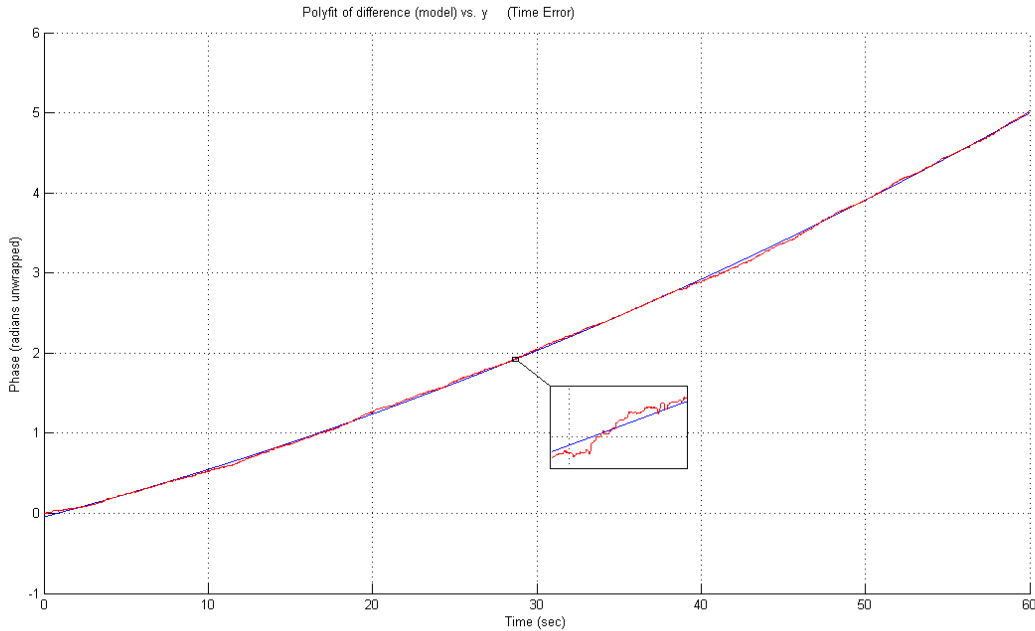


Figure 5.9: Model of relative phase between channels

In figure 5.9, the model from equation 5.17 is compared, i.e. $\frac{\varphi_2(t) - \varphi_1(t)}{2\pi f_0}$ is compared to $a_2 - a_1 + (b_2 - b_1)t + (c_2 - c_1)t^2$. The relative phase model between the two channels is a great deal smaller, thus from figure 5.9, the random phase noise can be seen. Though with the phase noise present, the model is still fairly accurate. These results show a relative frequency offset of $b \simeq 0.0033$, corresponding to a frequency offset of approximately 33Hz for these experimentations. The frequency drift is typically approximated to $Dr \simeq 7.346 \times 10^{-8}$, which closely resembles the predictions in table 4.2 for short-term stability. Thus, this corresponds to a frequency drift of approximately 0.001469Hz/second. These results will be used in chapter 6 to investigate these effects on the radars performances.

5.5 Summary

This chapter introduces the concepts of time and frequency characterization. Linear drifts in frequency can effect the performances of oscillators and thus the performances of the system. This chapter focuses on the phase by regressing it to a quadratic $(a + bt + \frac{Dr}{2}t^2 + \varepsilon(t))$. This model contains coefficients of the time error, frequency offset and frequency drift, as well random variations. The relative drift between two channels, and the state of oscillators over long periods is discussed

and formulated so that predictions of the drift within a system can be made.

A brief overview of the two-sample (Allan) variance is discussed, used to measure the deviations and stability of oscillators. It can also be used to estimate the intensity and power spectral density of noise, categorized into five power-laws (White PM, Flicker PM, White FM, Flicker FM and Random walk FM).

A stable GPSDO [14] is used in experimentation, showing models of the phase, including the relative phase models between channels.

Chapter 6

Effects of Oscillator Mismatch

6.1 Introduction

In chapter 5 the frequency characteristics was determined, through the phase, and modelled for predictions. This chapter will examine the effects of the model and predictions with respect to target detection through Doppler.

Coherence in radar applications is defined as whether the phase relationship (at the carrier frequency) between successive pulses are known and stable [21]. If a radar is coherent, then M successive pulses, from a non-fluctuating target, can be added. This summing will improve the radar's SNR by a factor of M . If the radar is not coherent, however, these pulses will not add in phase and summing will not improve the SNR. This is further discussed in [29] Furthermore, as the radar's probability of detection is related to the SNR, degradation of the radar's coherence will decrease the SNR. Thus, in coherent radars (PCL), the target detection capability decreases with an increase in phase noise of the frequency reference.

In bistatic radar configurations, the local oscillators in the receiver needs to be synchronized not only in frequency but also the phase offsets. The ability of these phase offsets to remain constant during target detection will influence the level of coherence, thus the level of coherency is dependent on the stability of the local oscillators.

6.2 Doppler Effect

The relationship between the range of the target and time for a monostatic radar is given by:

$$R = \frac{c\tau_d}{2} \quad (6.1)$$

Where:

- R is the range of the target from the radar
 τ_d is the round trip time delay of the signal between transmitter and receiver
 c is the propagation speed

In the case of a bistatic radar, the time delay is related to the range of the target by [9]:

$$\tau_d = \frac{R_T + R_R}{c} \quad (6.2)$$

where:

- R_T is the range of the transmitter to the target
 R_R is the range of the target to the receiver

Thus, from equation 6.1 and 6.2, the radar's range accuracy is directly proportional to the error in the timing signal, as an error in τ_d is directly proportional to an error in R , for a monostatic radar and proportional to an error in $R_T + R_R$ for a bistatic radar.

In a Doppler radar, the signal received from the moving target, by the radar, differs in frequency from the transmitted frequency and thus differs in phase too, by an amount that is proportional to the radial component of the velocity relative to the radar. This Doppler shift is given in equation 2.1, for a monostatic case, as:

$$f_d = \frac{2v_r}{\lambda}$$

and for a bistatic case, given by equation 2.2 as:

$$f_d = -\frac{1}{\lambda} \frac{d(R_T + R_R)}{dt}$$

which may be rewritten as:

$$f_d = \frac{f_0}{c} \frac{d(R_T + R_R)}{dt} \quad (6.3)$$

Thus, by combining equation 6.2 and 6.3, The Doppler frequency becomes:

$$f_d = f_0 \frac{d\tau}{dt} \quad (6.4)$$

This shows that the Doppler shift is equal to a change in phase and group delay corresponding to the change in range. As a result the velocity of the target and the radar frequency are primarily

determinants of the phase noise requirements [26].

6.3 Cross-Correlation

As discussed in section 2.2.1, cross-correlation is the measure of similarity of two waveforms as a function of time-lag applied to one of them. In passive radar the cross-correlation process is used to determine the Doppler-shifted and time-delayed echoes of the targets [22]. This process acts as a matched filter for the radar system, maximizing the SNR, thus providing the necessary signal processing gain to allow detection of the target echo. This process is also used to estimate the range and Doppler shift of the target.

The range-Doppler estimation is illustrated in figure 6.1 below:

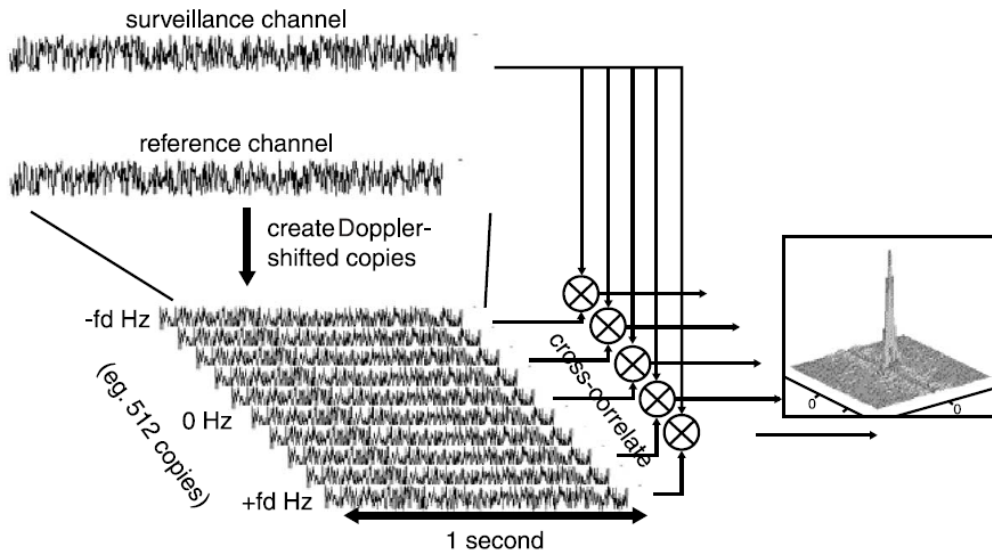


Figure 6.1: Concept of cross-correlation [22]

The algorithm of the concept shown in figure 6.1 operates on a one second sample of data. The reference signal is generated with several Doppler-shifted copies that acts as a bank of filter, each matched to a different target velocity. This operation can be written in the discrete time notation as [22]:

$$|\Psi(\tau, \nu)| = \left| \sum_{n=0}^{N-1} e(n) d^*(n - \tau) e^{j2\pi\nu n/N} \right| \quad (6.5)$$

where:

Ψ	is the amplitude-range-Doppler (ARD)
$e(n)$	is the filtered echo signal
$d(n)$	is the reference signal
τ	is the time delay corresponding to the bistatic time difference of arrival
ν	is the Doppler shift of interest

This algorithm only allows for a limited number of ranges, but all Doppler shifts are possible and only limited by the sample rate. The effects of cross-correlating signals that have a frequency offset and frequency drift will be shown in the following results.

6.4 Results

Using a radar simulator called FERS (the flexible, extensible radar and sonar simulator) [8], designed by M. Brooker, a PCL radar system will be simulated. This simulator includes a broadcast transmitter, two receivers on the same location and a moving aircraft. The two receivers will model the separate channels of a passive radar receiver. The reference channel of the receiver is modelled by a yagi antenna pointing directly at the transmitter, and the target return channel is modelled by an isotropic antenna. The isotropic antenna will receive both the reference signal from the transmitter as well as the echo signal, reflected off the target, thus it is necessary to cancel out the reference signal from the isotropic receiver.

Figure 6.2 illustrates the cross-correlations of ideal reference signals with ideal echo signals. Thus, there is no frequency offset or drift between the signals. For better view of the results, a colour contour mapping is used¹.

Figure 6.3 shows that the surveillance channel will also receive the reference signal. The reference signal is centred at zero frequency with no delay. The echo signal is seen at a higher frequency and delay, thus estimations of the targets range and Doppler shift can be made.

To demonstrate the effects of a frequency shift and frequency drift, models will be slightly exaggerated. Thereafter realistic models based on predictions made in chapter 5 will be shown.

Figure 6.4 illustrates the effect of a frequency offset of 10Hz. This offset introduces errors in the results, as it can be seen that both the reference and echo signals have been shifted. This shift will result in errors when estimating the targets range and Doppler shift.

Although this unrealistic model was made in figure 6.5, with a frequency drift of 10Hz/second, it is seen that frequency drifts greatly influences the results. Not only does it introduce a shift in the signals but also additional phase noise is introduced. This decreases the SNR, resulting in errors and

¹Refer to appendix for further illustrations.

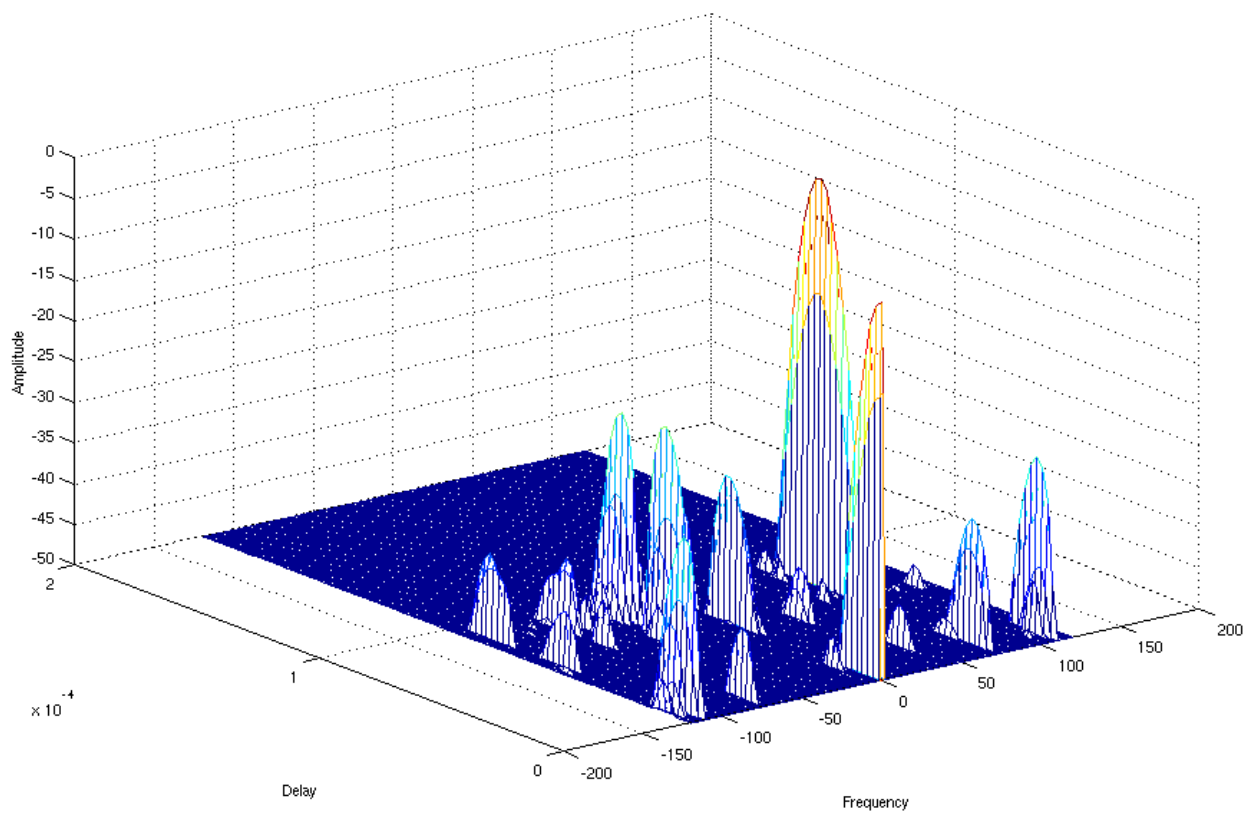


Figure 6.2: Cross-correlation of the reference and echo signals

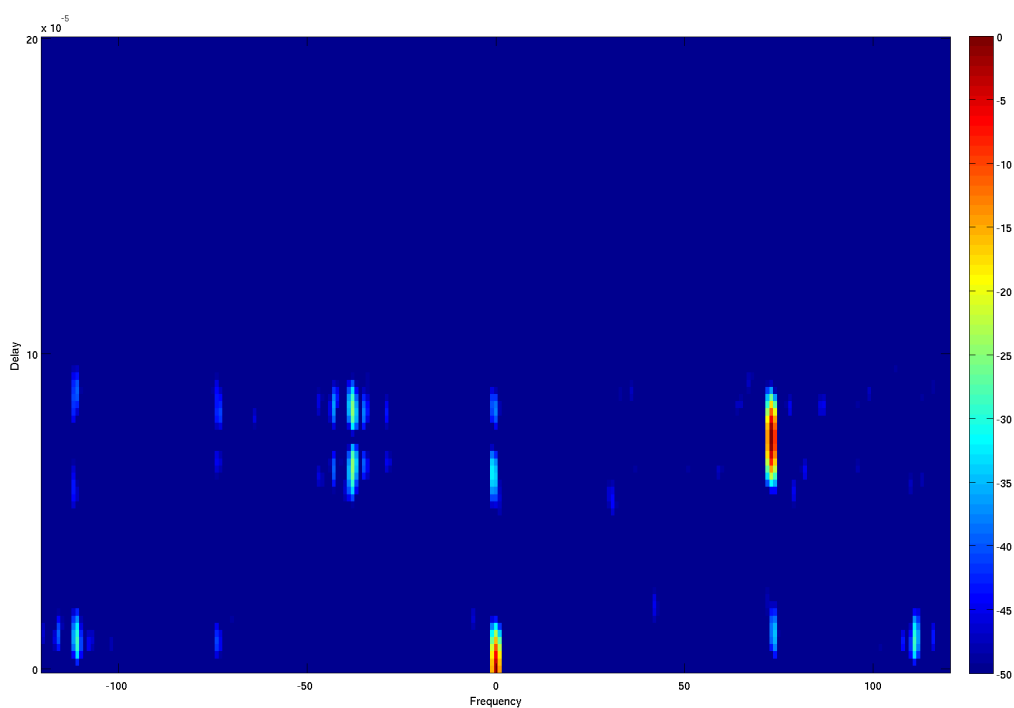


Figure 6.3: Colour map of ideal signal cross-correlation

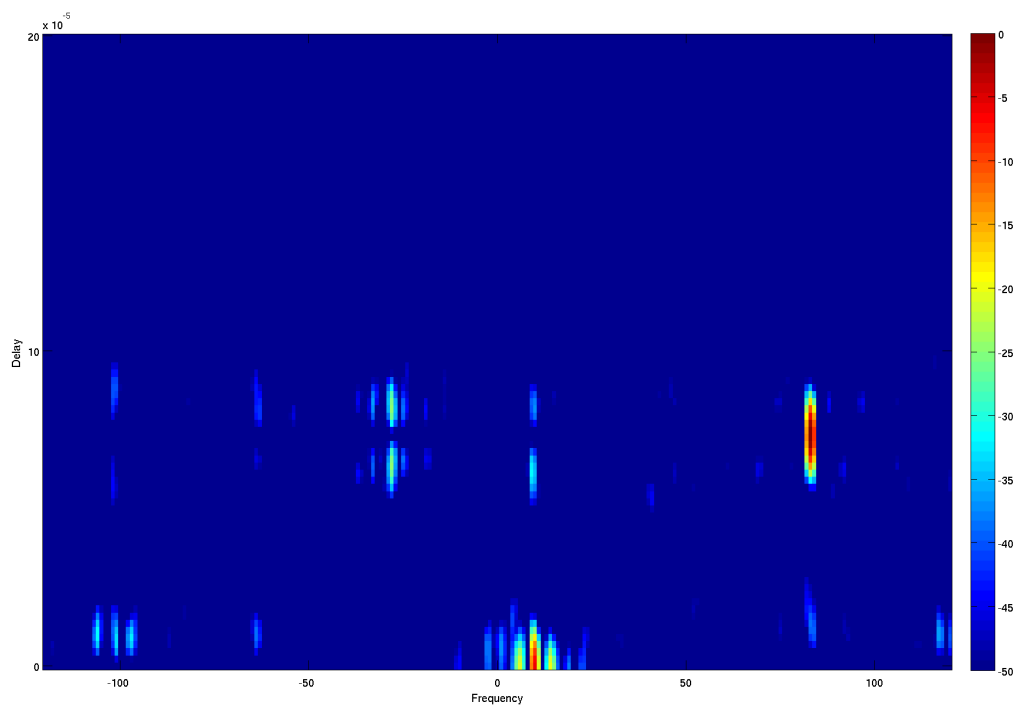


Figure 6.4: Effects of frequency offset

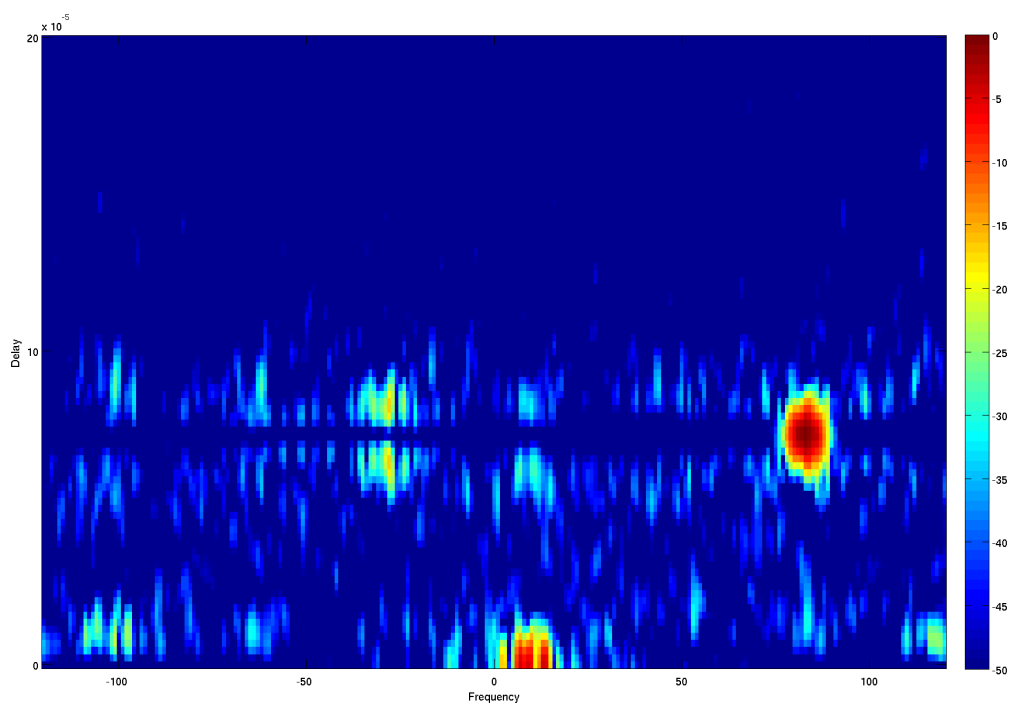


Figure 6.5: Effects of frequency drifts

reduced accuracy of the target detection process.

Using the results obtained in section 5.4, with the predictions of frequency offset and drift, the following results were obtained.

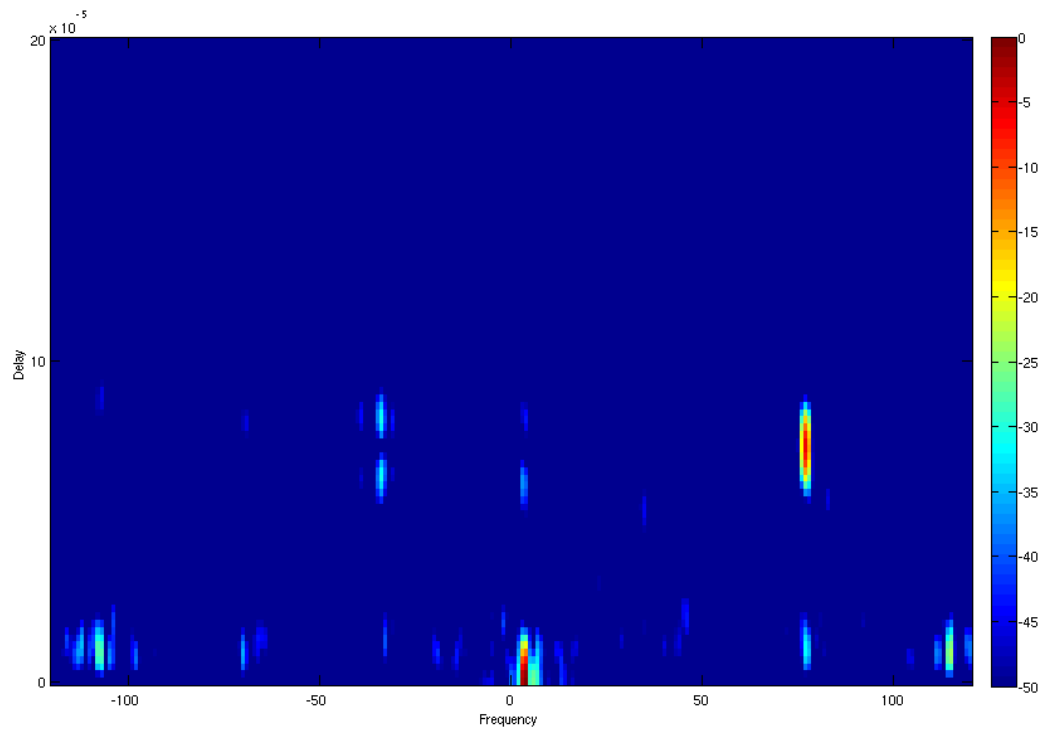


Figure 6.6: Actual results based on predictions

Figure 6.6, shows the effects of the predicted model. It can be seen that there is a shift in frequency and as well as some phase noise present, due to the drift.

6.5 Summary

Through radar and Doppler theories it can be seen that the radar's range accuracy is directly proportional to the errors in the timing signal. Errors in τ_d is directly proportional to an error in $R_T + R_R$ for bistatic radar configurations. In bistatic radars the Doppler shift is equal to a change in phase and group delay corresponding to the change in range, thus target velocity and radar frequency are primarily determinants of the phase noise requirements.

Cross-correlation is used to determine the Doppler-shifted and time-delayed echoes of the target. A matched filter bank process is used in passive radars to maximize SNR and thus estimate the range

and Doppler shift of the target.

Frequency offset and frequency drifts effects the results of the cross-correlation process, introducing error. This error introduces shifts in the cross-correlation process. Furthermore, the SNR is reduced and thus accuracy is compromised. This inevitably effects the performances of the radar's ability to accurately detect and track targets.

Chapter 7

Conclusions and Future Work

This research project investigates the effects of frequency drift and instabilities in the performances of Passive Coherent Location radar systems. Methods of characterization is discussed and used for the predictions of frequency offset and drifts over a specified time duration.

Frequency drifts are mainly caused by the performances of oscillators, such as local oscillators in mixers, used for frequency conversion. Thus, much of this thesis is based on oscillators, its properties and performances. Focus was made on quartz crystal oscillators due to the fact that the oscillators within the TVRX daughter boards, used in experimentations, is a 4MHz quartz crystal oscillator. The main factor affecting the performances of an oscillator is temperature. This has been compensated with the developments of different types of oscillators such as RTX0, TCXO and OCXO.

To determine the properties of the frequency, it is best to look at the phase of the frequency. By doing so, stability characterization methods can be applied. The most typical method ($x(t) = a + bt + \frac{Dr}{2}t^2 + \varepsilon(t)$) can model the variations in the phase quite accurately. This can then be used to predict the frequency drift and offsets. For short-term characterization, it is difficult to predict a typical drift, due to the fact that for short-term cases, drift is highly dependent on systems conditions and random fluctuations. Short-term characterization needs to be done periodically, over short time durations (typically seconds).

These instabilities, and thus frequency drifts, improves over time. Long-term characterization can vary from days to years. Very low sampling frequencies is required to reduce strenuous processing. For long-term it is also necessary to investigate phase noise, because long periods are dominated by flicker FM and random walk FM.

For future work, longer measurements can be made to determine long-term drift. This project focused on the short-term drift due to the large amounts of data gathered from measurements, thus

long term characterization was difficult to process. Correction of the drift can be made either post processing of the signal, thus introducing a feedback system, or done internally through the FPGA by applying adaptive processes, such as implementing a least-mean-square adaptive filter.

Appendix A

Frequency Measurements

Table A.1 shows measurements of the relative differences in frequency between two channels. Measurements were taken at hourly periods. Measurements of 1 second every minute for 30 minutes. Figure A.1 and A.2 shows the relative frequencies at time 10:45am and 11:45am respectively.

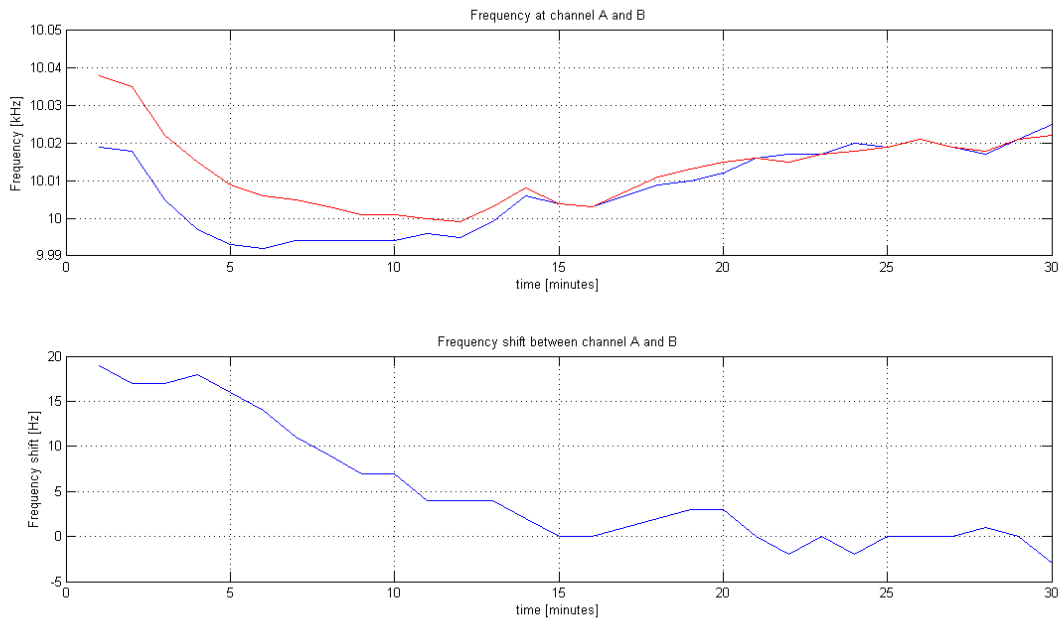


Figure A.1: Relative frequency during 10:45 am

Time (min)	Relative Shift (Hz)		
	10:45 AM	11:45 AM	12:45 AM
1	19	21	12
2	17	20	13
3	17	19	13
4	18	17	13
5	16	16	12
6	14	14	11
7	11	12	6
8	9	9	3
9	7	7	0
10	7	4	-3
11	4	3	-6
12	4	2	-7
13	4	1	-10
14	2	0	-9
15	0	-1	-10
16	0	-3	-9
17	1	-4	-10
18	2	-5	-10
19	3	-6	-9
20	3	-6	-7
21	0	-5	-4
22	-2	-5	-5
23	0	-6	-5
24	-2	-7	-7
25	0	-8	-7
26	0	-6	-7
27	0	-6	-8
28	1	-6	-8
29	0	-7	-5
30	-3	-7	-7

Table A.1: Measurement of frequency shifts

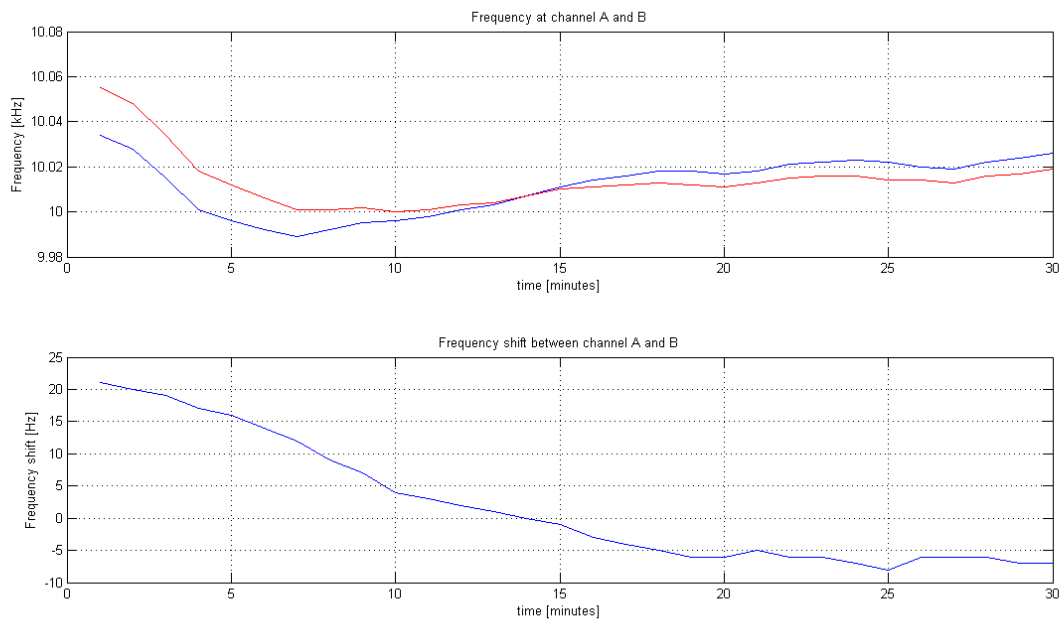


Figure A.2: Relative frequency during 11:45 am

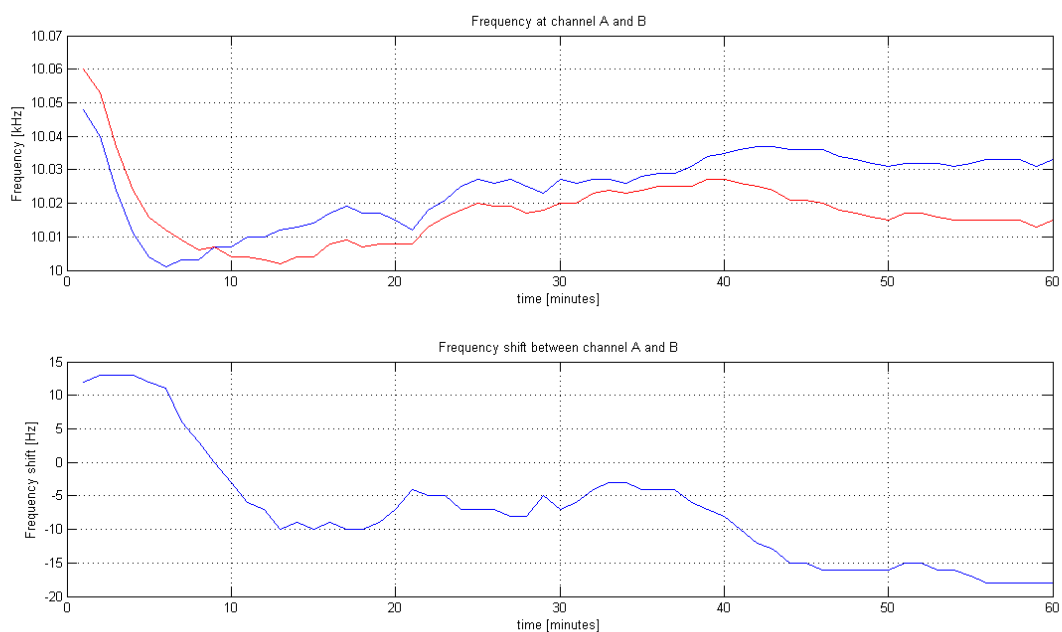


Figure A.3: Relative frequency over 1hr measurement

Appendix B

Cross-Correlation Plots

The following figures illustrate the cross-correlation between the reference signals and the echo signals, as well as the contour plots of the cross-correlation.

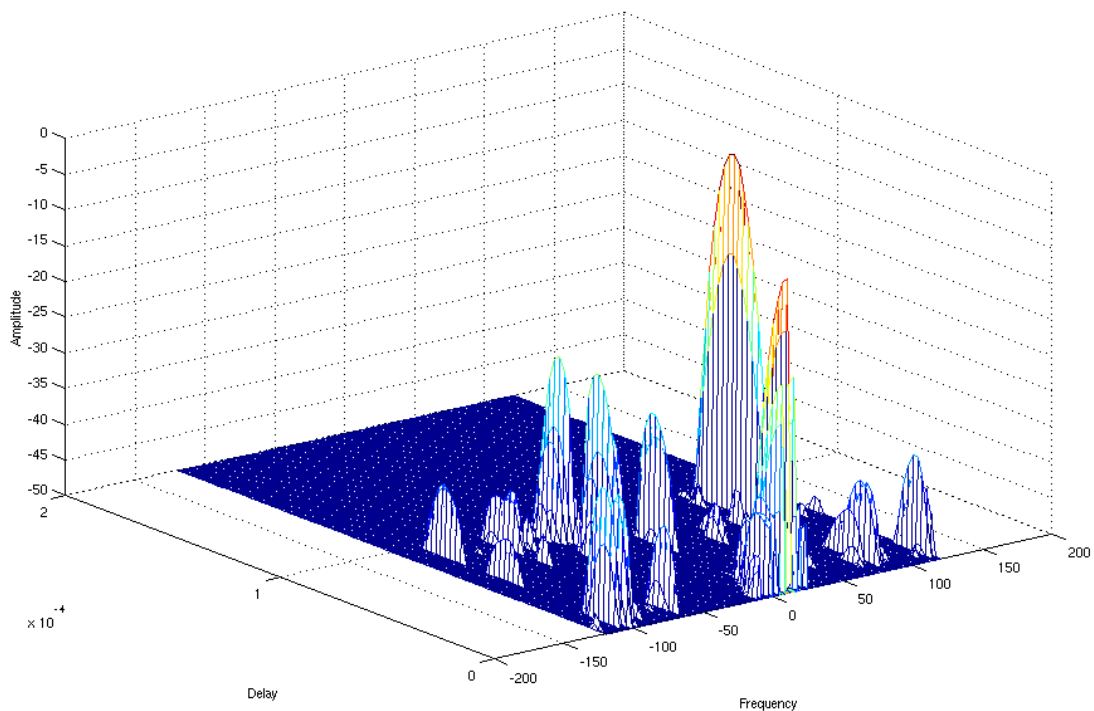


Figure B.1: Cross-correlation with frequency offset

It can be seen from these figures that a frequency offset will shift the reference frequency, and a frequency drift will introduce noise, thus degrading the accuracy.

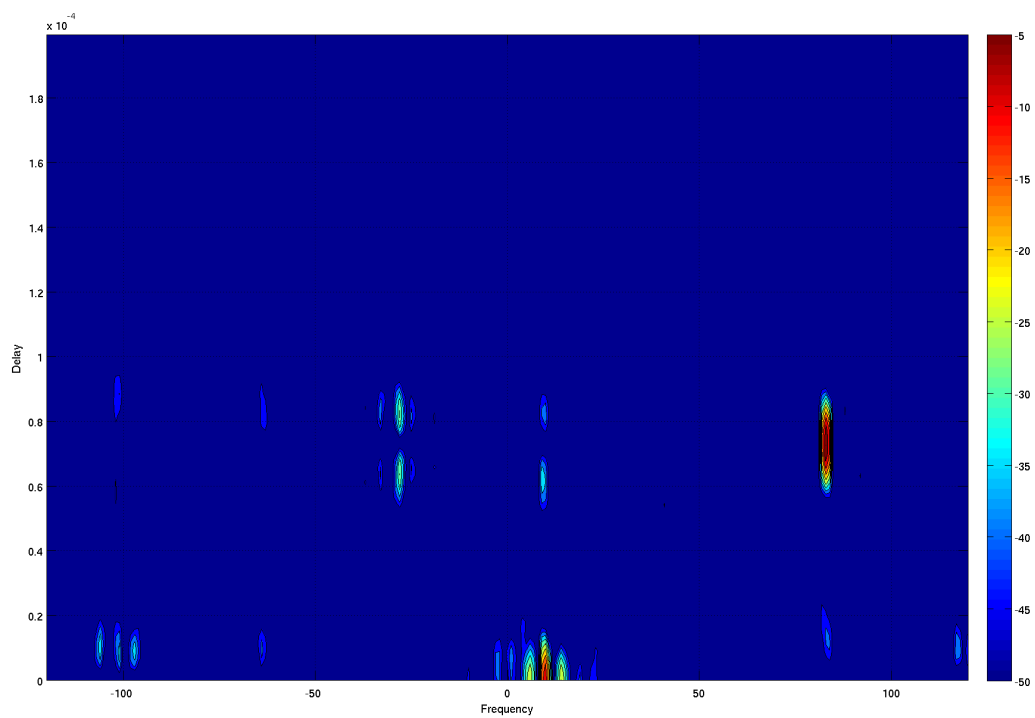


Figure B.2: Contour plot with frequency offset

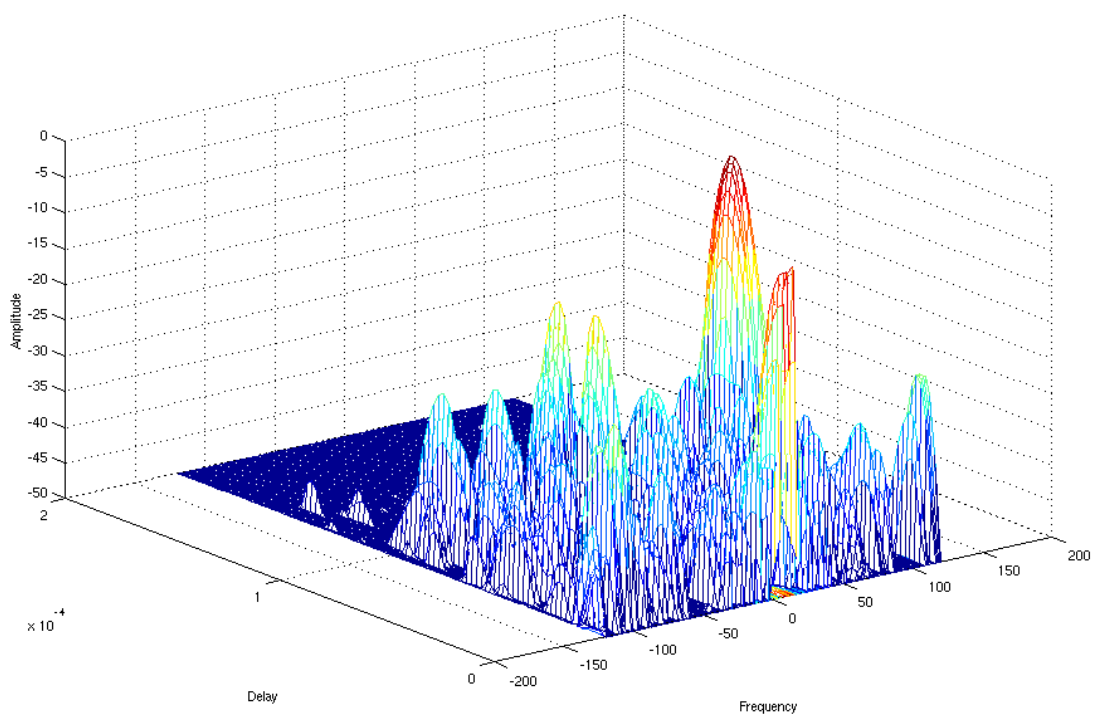


Figure B.3: Cross-correlation plot with frequency drift

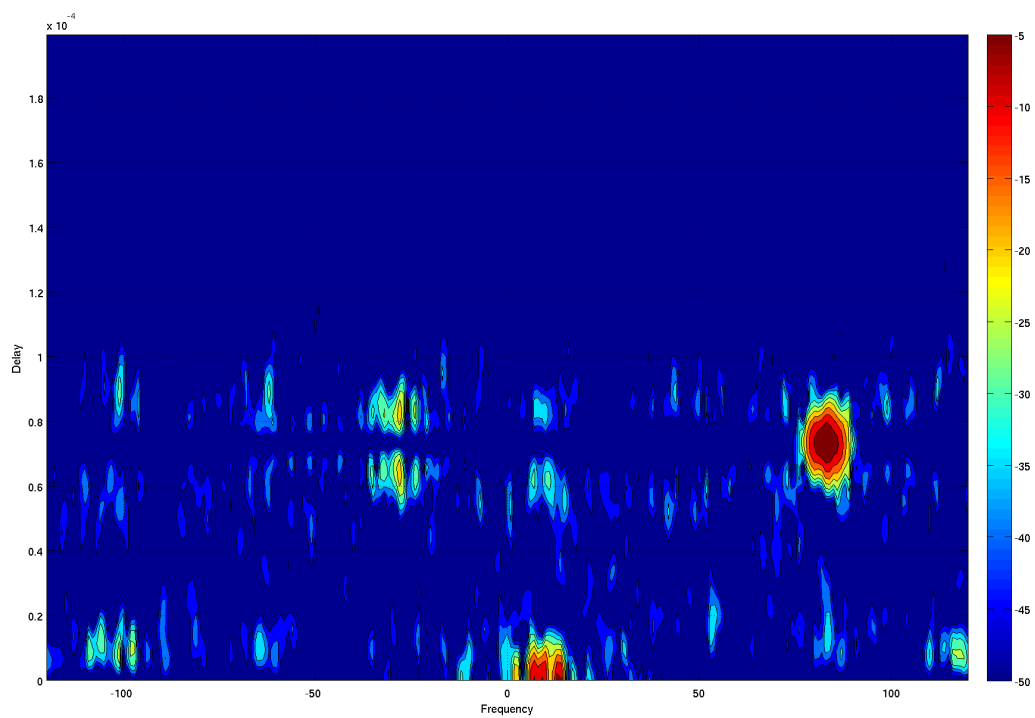


Figure B.4: Contour plot with frequency drift

Appendix C

Images of Equipment

The images of the equipment is shown in this Appendix.

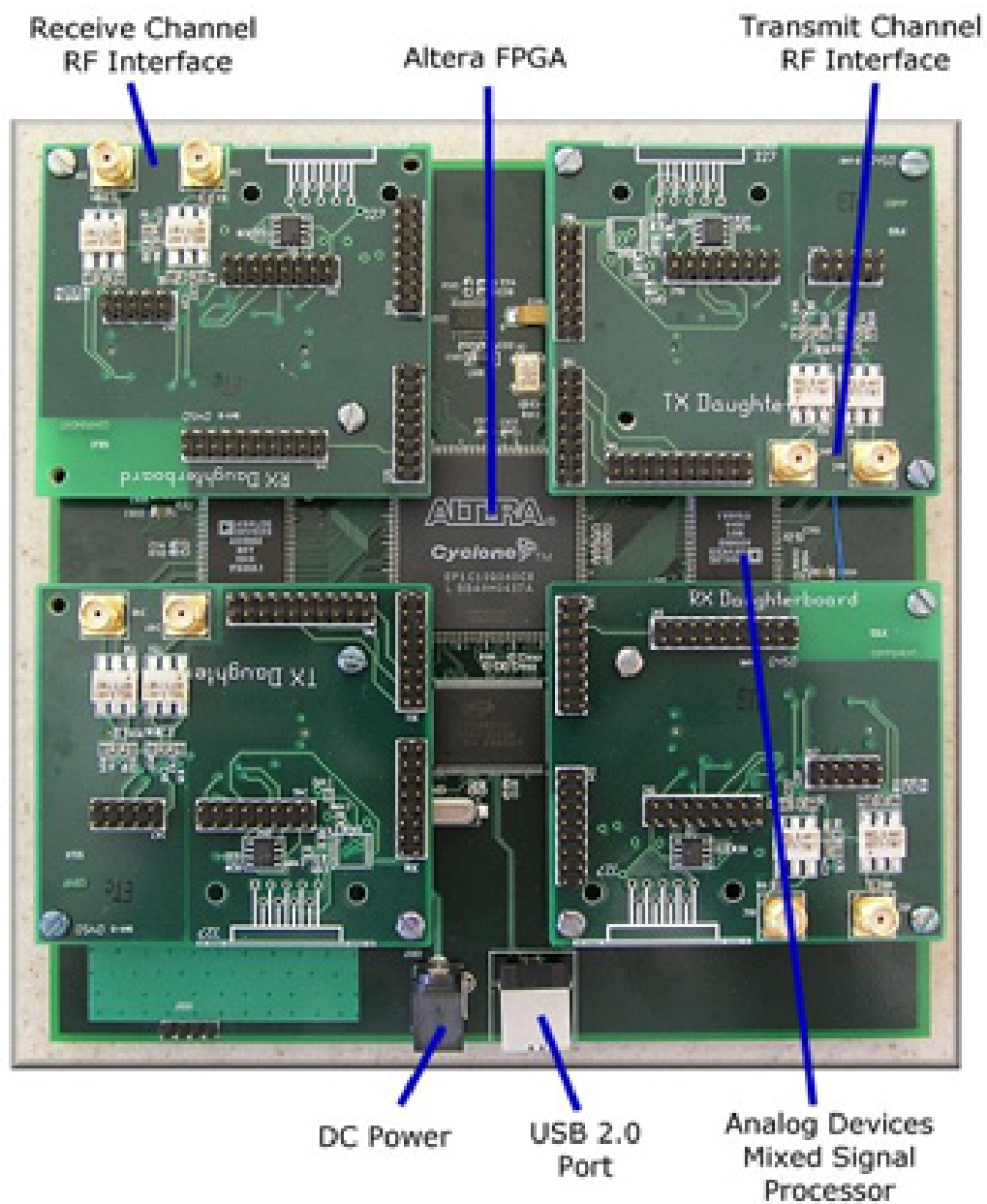


Figure C.1: USRP board



Figure C.2: USRP with TVRX Daughter boards



Figure C.3: USRP and signal generator



Figure C.4: USRP and GPSDO

Appendix D

Software Codes

All coding scripts written and used for this research project may be found in the CD provided.

D.1 Python codes

rx_file2.py

This script was written by A. Volkwin. This allows the USRP operate two receiver, capturing data for 1 second every minute for 30 minutes.

rx_file2_mod.py

This is the same as rx_file2.py, but is made to capture data for 1 minute continuously.

D.2 Matlab codes

read_complex_binary.m

This is used to read the files that the USRP outputs. The USRP outputs a binary file, and read_complex_binary is use to read this data.

freqshift_measurement.m

This measures the frequency shift, and plots the fft of the signals. This was provided by A. Volkwin.

plotfft2.m

Used to plot the fft.

bandpass_filter.m

Design of a bandpass filter

freq_15e6.m

The code is used to process the continuous sampling for 1 minute.

freq_15e6_mod.m

This is same as freq_15e6.m, to process the data for 1minute with the addition of splitting the 1minute into 1second plots.

freq_drift.m

This program processes the data and plots the fft of the 1st second and last second, thus the peaks of the fft's can be used to see the drift.

freq_drift_mod.m

This is similar to freq_drift.m but plots for 100ms instead of 1 second.

regression.m / regression_mod.m

This programs is used to characterize the frequency and phase. This will give coefficients of time offset, frequency offset and frequency drift. It uses the **polyfit** function in Matlab to do so.

using_allan.m

This program is uses allan.m, which was written by M. Brooker.

D.3 FERS Simulator [8]

drift.fersxml

This simulates two receivers, both located on the origin, with one yagi antenna pointing at the transmitter, and a isotropic antenna. A transmitter is located on a separate site, and an moving aircraft is simulated. In this program it is possible the model the drift and frequency offsets, as well as the phase noise.

Bibliography

- [1] D. W. Allan. *Time and Frequency (Time Domain) Characterization, Estimation, and Prediction of Precision Clocks and Oscillators*. 1987.
- [2] J. A. Barnes; R. H. Jones; P. V. Tyron; D. W. Allan. *Stochastic Models for Atomic Clocks*. 1983.
- [3] H.D. Griffiths; C.J. Baker. *Measurement and Analysis of Ambiguity Functions of Passive Radar Transmissions*. 2005.
- [4] H.D. Griffiths; C.J. Baker. Passive coherent location radar systems. part 1: Performance prediction. *IEE Proceedings*, 152, 2005.
- [5] A. Ballato. *Precision Frequency Control. Volume 2: Oscillators and standards*. Academic Press, Inc, 1985.
- [6] J. A. Barnes. *The Measurement of Linear Frequency Drift in Oscillators*. 1983.
- [7] E. Blossom. Gnu radio: Tools for exploring the radio frequency spectrum. *Linux Journal*, 2004.
- [8] M. Brooker. *FERS-The flexible,extensible radar and sonar simulator*. 2007.
- [9] M. Brooker. *The Design and Implementation of a Simulator for Multistatic Radar Systems*. 2008.
- [10] A. Guner; M. Temple; R. Claypoole. *Direct path filtering of DAB Waveform from PCL Receiver Target Channel*. 2003.
- [11] B. A. Fette. *RF and Wireless Technologies*. 2007.
- [12] E. Hanle; Dr. Ing; H. Gunpath. Survey of bistatic and multistatic radar. *IEE Proceedings*, pages 587–595, 1986.
- [13] P.E. Howland. *A Passive Metric Radar Using the Transmitter of Opportunity*. 1994.
- [14] J.S. Sandenbergh; M.R. Inggs. *A Common View GPSDO to Synchronize Netted Radar*. 2007.

- [15] M.C. Jackson. *The Geometry of Bistatic Radar Systems*. 1986.
- [16] J. M. Kristensen. Gnu radio: An introduction.
- [17] G. Kamas; M.A. Lombardi. *Time and Frequency Users Manual*. 1990.
- [18] Z. Peyton; Jr. Peebles. *Radar Principles*. John Wiley & Sons, 1998.
- [19] D. M. Pozar. *Microwave and RF Design of Wireless Systems*. John Wiley & Sons, Inc, 2001.
- [20] GNU Radio. Gnu radio: The gnu software radio. August 2008. URL <http://www.gnu.org/software/gnuradio/index.html>.
- [21] H.J. Reed. *Software Radio: A Modern Approach to Radio Engineering*. 2002.
- [22] P.E. Howland; D. Maksimiuk; G. Reitsma. *FM Based Bistatic Radar*. 2005.
- [23] J M Rueger. *Quartz Crystal Oscillators and Their Effects on the Scale Stability and Standardization of Electronic Distance Meters*. 1982.
- [24] J.S. Sandenbergh. *A GPS synchronised, Quart Crystal Frequency Standard*. 2005.
- [25] D. A. Scaperoth. Configuration sdr operation for radio applications using gnu radio and the universal software radio peripheral. Master's thesis, Virginia Polytechnic Institute and State University, 2007.
- [26] Schoenenberger. *Principles of Independent Receivers for use with Cooperative Radar Transmitters*. 1982.
- [27] M. Skolnik. *Introduction to Radar Systems*. 1962.
- [28] J. Zhu; Y. Hong; L. Tao. Adaptive beamforming passive radar based on fm radio transmitter.
- [29] A. Volkwin. Suitability of a commercial software defined radio system for passive coherent location. Master's thesis, University of Cape Town, 2008.
- [30] W. Wang. *Approach of Adaptive Synchronization for Bistatic SAR Real-Time Imaging*. 2007.
- [31] M. Weiss. *Synchronisation of Bistatic Radar Systems*. 2004.
- [32] N.J. Willis. *Bistatic Radars and Their Third Resurgence: Passive Coherent Location*. 2002.
- [33] N.J. Wills. *Bistatic Radar*. 1995.